# SYNTHESIS OF ZINC OXIDE NANOROD FROM ZINC BORATE FOR SUPERCAPACITOR ELECTRODE

**2022**
**MASTER THESIS**
**METALLURGY AND MATERIALS ENGINEERING**

**Chikh Sidi El Mokhtar Mohamed LEFDHIL**

**Thesis Advisor**
**Assist. Prof. Dr. Safa POLAT**

# SYNTHESIS OF ZINC OXIDE NANOROD FROM ZINC BORATE FOR SUPERCAPACITOR ELECTRODE

**Chikh Sidi El Mokhtar Mohamed LEFDHIL**

**T.C.**
**Karabuk University**
**Institute of Graduate Programs**
**Department of Metallurgy and Materials Engineering**
**Prepared as**
**Master Thesis**

**Thesis Advisor**

**Assist. Prof. Dr. Safa POLAT**

**KARABUK**

**December 2022**

I certify that in my opinion the thesis submitted by Chikh Sidi El Mokhtar Mohamed LEFDHIL titled "SYNTHESIS OF ZINC OXIDE NANOROD FROM ZINC BORATE FOR SUPERCAPACITOR ELECTRODE " is fully adequate in scope and in quality as a thesis for the degree of Master of Science.

Assist. Prof. Dr. Safa POLAT .....
Thesis Advisor, Department of Metallurgy and Materials Engineering

This thesis is accepted by the examining committee with a unanimous vote in the Department of Metallurgy and Materials Engineering as a Master of Science thesis. December 26, 2022

| Examining Committee Members (Institutions) | Signature |
|---|---|
| Chairman : Assoc. Prof. Dr. Fatih AYDIN (KBU) | ..... |
| Member : Assoc. Prof. Dr. Adem YAR (BU) | Online |
| Member : Assist. Prof. Dr. Safa POLAT (KBU) | ..... |

The degree of Master of Science by the thesis submitted is approved by the Administrative Board of the Institute of Graduate Programs, Karabuk University.

Doç. Dr. Müslüm KUZU .....
Director of the Institute of Graduate Programs

*"I declare that all the information within this thesis has been gathered and presented in accordance with academic regulations and ethical principles and I have according to the requirements of these regulations and principles cited all those which do not originate in this work as well."*

Chikh Sidi El Mokhtar Mohamed LEFDHIL

## ABSTRACT

**M. Sc. Thesis**

**SYNTHESIS OF ZINC OXIDE NANOROD FROM ZINC BORATE FOR SUPERCAPACITOR ELECTRODE APPLICATION**

**Chikh Sidi El Mokhtar Mohamed LEFDHIL**

**Karabuk University**
**Institute of Graduate Programs**
**Department of Metallurgy and Materials Engineering**

**Thesis Advisor:**
**Assist. Prof. Dr. Safa POLAT**
**December 2022, 70 pages**

This thesis is planned to synthesize zinc oxide from zinc borate mineral to use it as electrode material in supercapacitors. For this purpose, firstly, zinc borate mineral was treated with hydrochloric acid at different concentrations, and the extracted zinc metal concentration was optimized. Concentrations were measured by atomic absorption spectroscopy (AAS). Then, direct zinc oxide synthesis was carried out by hydrothermal method on the nickel foam surface using the solution with the highest zinc content. After synthesis, the products were characterized in terms of crystal structure, chemical bond, and geometric shape by XRD, FTIR, and SEM analyses. The results showed that zinc oxide nanorods with an average size of 358 nm were successfully synthesized on the nickel foam surface. The synthesized electrode was then subjected to cyclic voltammetry (CV) and galvanostatic charge-discharge (GCD) tests. These measurements showed that the electrode has a battery-type charge storage

character, and the highest specific capacitance is approximately 527 mF/cm$^2$ at a current density of 1 mA/cm$^2$. In addition, the energy and power densities of zinc oxide-based electrodes were calculated as 11 mWh/cm$^2$ and 200 mW/cm$^2$ at a current density of 2 mA/cm$^2$, respectively. Although these results are single-component compared to their counterparts in the literature, it is concluded that they are quite promising.

**Key Words:** Zinc borate, zinc oxide, nanorod, supercapacitor, extraction, hydrothermal method.
**Science Code :** 91520, 91530

# ÖZET

**Yüksek Lisans Tezi**

## ÇİNKO BORATTAN ÇİNKO OKSİT NANOÇUBUK ÜRETİMİ VE ELEKTROKİMYASAL ÖZELLİĞİNİN İNCELENMESİ

**Chikh Sidi El Mokhtar Mohamed LEFDHIL**

**Karabük Üniversitesi**
**Fen Bilimleri Enstitüsü**
**Metalurji ve Malzeme Mühendisliği Anabilim Dalı**

**Tez Danışmanı:**
**Dr. Öğr. Üyesi Safa POLAT**
**Aralık 2022, 70 sayfa**

Bu tez çalışmasında çinko borat mineralinden süperkapasitörlerde elektrot malzemesi olarak kullanılması amacıyla çinko oksit sentezlenmesi planlanmıştır. Bu amaçla ilk olarak çinko borat minerali farkı derişimlerde hidroklorik asit ile muamele edilmiş ve ekstrakt edilen çinko metali konsantrasyonu optimize edilmiştir. Konsantrasyonlar atomik absorpsiyon spektroskopisi (AAS) ile ölçülmüştür. Daha sonra en yüksek çinko içerikli solüsyon kullanılarak nikel foam yüzeyinde hidrotermal yöntemle doğrudan çinko oksit sentezi gerçekleştirilmiştir. Sentez sonrası ürünler XRD, FTIR ve SEM analizleri ile kristal yapı, kimyasal bağ ve geometrik şekli bakımından karakterize edilmiştir. Elde edilen sonuçlar nikel foam yüzeyinde ortalama 300 nm boyutunda çinko oksit nano çubuklarının başarılı bir şekilde sentezlendiğini göstermiştir. Bu işlemlerin ardından sentezlenen elektrotun çevrimli voltametre (CV) ve galvano statik şarj-deşarj (GCD) ölçümleri de gerçekleştirilmiştir. Bu ölçümler elektrotun pil tipi şarj depolama karakterine sahip olduğunu ve en yüksek spesifik kapasitansının ise 1

mA/cm$^2$ akım yoğunluğunda yaklaşık 527 mF/cm$^2$ olduğunu göstermiştir. Ayrıca bu elektrotun 1 mA/cm$^2$ akım yoğunluğundaki enerji ve güç yoğunlukları da sırasıyla 11.2 mWh/cm$^2$ ve 200 mW/cm$^2$ olarak hesaplanmıştır. Bu sonuçlar literatürdeki muadillerine kıyasla tekli bileşen olmasına rağmen oldukça umut vaat edici olduğu sonucuna varılmıştır.

**Anahtar Kelimeler :** Çinko borat, çinko oksit, nano çubuk, süper kapasitör, ekstraksiyon, hidrotermal yöntem.

**Bilim Kodu** **:** 91520, 91530

## ACKNOWLEDGMENT

I would like to thank the all-powerful God for providing me with the fortitude I required to accomplish my research.

My profound appreciation goes out to my advisor, Dr. Safa Polat, for his genuine interest in and assistance with the thesis. Working and learning under his supervision was an honor and a pleasure.

In addition, I would like to thank the other graduate students from the Nano Energy laboratory, Muwafaq Mashrah, El Moctar Mohamed, Mariem Abdi, and Mariem Mohamed El Mamy, who helped me operate the laboratory's equipment.

In addition, I would like to thank my family Mom, Dad, Mohamed, and Raya along with my uncle Horma Hamoud and my friend Majid Deidah for their support and guidance thus far.

I am happy that the Materials Research and Development Center (MARGEM) at the Iron and Steel Institute of Karabuk University let me to utilize their laboratories.

Also acknowledged is the Karabuk University Scientific Research Projects Unit (KBU-BAP), whose KBÜBAP-21-ABW-047 project supported the analysis.

**CONTENTS**

**Page**

**Page**

## LIST OF FIGURES

**Page**

## LIST OF TABLES

**Page**

## SYMBOLS AND ABBREVITIONS INDEX

### SYMBOLS

| | |
|---|---|
| A | : Ampere |
| mA | : Milliampere |
| µm | : Micrometer |
| g | : Gram |
| mg | : Milligram |
| $cm^3$ | : Centimeter cubic |
| L | : Liter |
| °C | : Degrees Celsius |
| K | : Kelvin |
| s | : Second |
| Zn | : Zinc |
| ZnO | : Zinc Oxide |
| $ZnCO_3$ | : Zinc carbonate |
| $MgCl_2$ | : Magnesium chloride |
| KCl | : Potassium chloride |
| CaCl | : Calcium chloride |
| mF | : Millifarad |
| $mWh/cm^2$ | : Milliwatts hour per centimeter squared |
| $mW/cm^2$ | : Milliwatts per centimeter squared |
| $CuFeS_2$ | : Chalcopyrite |
| $SO_2$ | : Sulfur dioxide |
| $CO_2$ | : Carbon dioxide |
| Cl | : Chloride |
| S | : Sulphur |

**ABBREVITIONS**

Ca : Specific capacitance

E : Energy density

CVD : Chemical vapor deposition

PVD : Physical vapor deposition

M : Molar

SEM : Scanning Electron Microscope

XRD : X-Ray Diffraction

XPS : X-ray photoelectron spectroscopy

FTIR : Fourier Transform Infrared Spectroscopy

AAS : Atomic absorption spectroscopy

P : Power density

CFO : Copper ferrite (CuFe2O4)

GCD : Galvanostatic charge-discharge

GNPs : Graphene nanoplates

PVDF : Polyvinylidene difluoride

NP : Nanoparticles

# PART 1

## INTRODUCTION

Supercapacitors, also known as ultracapacitors, are energy storage devices that have the ability to store large amounts of electrical energy [1]. They have a high capacitance, often in the range of thousands of Farads, making them significantly different from traditional capacitors [2]. They have several advantages over batteries, such as faster charging and discharging times, longer lifespan and wider temperature range, which makes them suitable for a variety of applications such as electric vehicles, portable electronics, and power tools. Supercapacitors are grouped into two types based on their method of charge storage, which are electrochemical double layer capacitors (EDLCs) and pseudocapacitors (PCs) [3]. Energy can be stored in EDLCs through the attachment and detachment of ions on the surface of the electrode and electrolyte interfaces, while PCs use quick and reversible chemical reactions between electrolyte ions and electroactive materials [3,4]. Generally, EDLCs have a longer service life but less specific energy storage compared to pseudocapacitors. Researchers are currently exploring different materials, such as metal oxides, carbon materials, and conductive polymers, to enhance the electrochemical performance of supercapacitors. A number of oxides and non-oxides among metallic compounds has gained widespread attention [3–5].

Metal oxides, such as zinc oxide (ZnO), have been extensively studied for their potential in a wide range of applications, including energy storage as a supercapacitor material. ZnO, specifically, has a high specific capacitance of around 470 F $g^{-1}$, which makes it a promising material for use in supercapacitors [6]. Its low-cost, earth-abundant and environmentally friendly properties make it a favorable material. ZnO can be synthesized in various forms such as nanoparticles, nanowires, and thin films, which increases the surface area and enhances the capacitance performance [7]. Additionally, ZnO has a good electronic conductivity which makes it suitable for

pseudocapacitors applications, where energy is stored by means of electrochemical reactions that occur on the surface of the electrodes [8]. ZnO also has excellent chemical stability, which is an important feature for energy storage devices. Furthermore, ZnO has a wide bandgap of 3.37 eV and a large exciton binding energy of 60 meV, which make it an ideal material for high-power, high-frequency applications [9].

Nanotechnology is an important field of science that has significantly changed many areas of our lives and is promising in a positive sense [10]. The components developed by this technology are divided into four classes 0D, 1D, 2D, and 3D [11]. This classification is related to the components' lengths of the x, y and z directions. When a component is smaller than 100 nm in all three directions, that is called 0D. If only one direction is greater than 100 nm, it is called 1D, if it has two dimensions greater than 2D, and if it is greater than three dimensions, it is called 3D [12].

In light of all of these predictions, the primary goal of this thesis research is to investigate the effects of different concentrations of HCl during the extraction of Zn from zinc borate. In this regard, the concentrations of zinc in the solutions after the extraction process were measured using atomic absorption spectroscopy (AAS), and the results were evaluated. The most concentrated solution was then chosen, and it was used for synthesizing zinc oxide supercapacitor electrode by the hydrothermal method on the nickel foam surface. The obtained products were characterized using FTIR, XRD, and SEM studies of chemical bonds, crystal structure, and microstructure. The electrochemical characterization was carried out using cyclic voltammetry (CV) and galvanostatic charge-discharge (GCD) in a three-electrode system to be used as electrode. Electrochemical results were than used for calculation of specific capacitance, energy and power density of zinc oxide electrodes. All these results were also evaluated by comparing in literature review.

# PART 2

# EXTRACTION PROCESS

## 2.1. METAL EXTRACTION METHODS

The metal extraction process incorporates a couple of stages, all of which anticipates that energy should carry out the requirement for three head capacities. Taking care of capacities incorporate decreasing assessment botches, mixing materials, moving them, fabricating them, and other mechanical endeavors that require electric power [13,14]. Extraction methods may be classed as pyrometallurgy or hydrometallurgy, and they can also entail physical separation and hybrid separation [15]. Pyrometallurgy is employed to increase slag stage regulation by injecting a thermal, causing precious metals in the slag to undergo physical or chemical conversion, allowing precious minerals and gangue to be segregated [16]. Pyrometallurgy comprises a wide range of procedures that may be used to various physical forms of slag. Several metals, particularly those susceptible to temp and atmosphere, such as Zn, Cu, Zr, Ti, Pb, and Ta, may be separated using it [17]. Moreover, increased roasting takes a lot of energy, and during the recovery process, a lot of high-heat exhaust gas and hazardous gases like CO are released. Leaching is a technique for dissolving precious metals in slag in solution or precipitating them out in a new solid phase. Inorganic leaching agents, such as acids, alkali metals, salts, or microbes, frequently are employed. Hydrometallurgy, as opposed to pyrometallurgy, consumes less energy and produces less pollutants [16]. Quasi metals, such as zinc, lead, and copper, have historically been obtained almost exclusively by the metallurgical processing of sulfide ores. This method has been in use for centuries. The persistent mining that has taken place in the sulfide ore deposits over the last several years has led to their gradual depletion, bringing in copious smelting residue and significant pollution from heavy metals [18].

Presently, the traditional hydrometallurgical method including oxidative roasting, acid leaching, purification, and electrowinning procedures is used to generate much more than 85 percent of all zinc produced worldwide. ZnS is changed into ZnO during the oxidative roasting process, although a sizeable portion combines with the iron contaminants to create zinc ferrite [18,19].

Significant minerals in zinc metals are sphalerite ZnS, zincite ZnO, franklinite ZnO $(Fe, Mn)_2O_3$, calamine $Zn_2OH_2\ SiO_3$ and smith stone $ZnCO_3$. Zinc minerals ordinarily are typically 5-15% zinc. Roughly 80% of zinc mines are underground, 8% are surface mined and the rest are a blend of the two minerals [20]. Zinc decontaminating is the process of converting zinc concentrates (zinc minerals) into pure zinc. The most well-known zinc concentrate is zinc sulfide, which is created by concentrating sphalerite using the froth lightness process [20]. Zinc sulfide is in like manner used to treat assistant (reused) zinc materials, similar to zinc oxide. Reused zinc addresses around 30% of outright zinc creation [13]. In the 95% of zinc hydrometallurgical procedures, zinc concentrate is transformed into zinc roasted in a calciner [22,23].

$$ZnS(s) + 1.5O_2(g) \rightarrow ZnO(s) + SO_2(g) \quad (1.1)$$

Equation 1.1 describes a gas-solid heterogeneous noncatalytic process that produces solids. The best suitable model to describe this response is the SUCM. The following equations (1.2), (1.3), and (1.4) are made in order to make the SUCM more appropriate for summarizing the reaction. Oxygen transmission out all over the environment liquid barrier integrity of the solid [22].

$$r_1 = 4\pi R^2_S\ k_{G,\,O2}\,(C_{O2,\,b} - C_{O2,\,s}) \quad (1.2)$$

The movement of oxygen into a sludge surface

$$r_2 = 4\pi R^2_C D_{e.}\ drC_{O2}/dry \quad (1.3)$$

Interaction of substances with the bulk material

$$r_3 = 4\pi R^2_C\ o_r\ C_{O2,\,s} \quad (1.4)$$

where $r_1$ is the speed at which oxygen diffuses through the liquid layer, $r_2$ is the frequency at which oxygen vaporizes through the solid surface, and $r_3$ is the rate at which chemicals interact on the level material. The radius of the solid particle and the unreacted core, correspondingly, is denoted by RS and RC, the oxygen level in the solid matrix and on the particle surface, correspondingly, are $CO_2$, b and $CO_2$, s. The mass transfer coefficient of the gas is kG, $O_2$. De is the effective diffusivity of oxygen over the gas film, kr is the sample mean of oxygen in the product layer, the RC's contact response [22,24].

## 2.2. ZINC MINERALS

Zinc is presently delivered from zinc sulfide minerals, which are the chief wellspring of zinc, and conventional buoyancy processes simplify it to isolate the sulfide minerals from the gangue [15]. Beneficiation of oxidized zinc minerals has developed progressively significant as of late as sulfur-bearing metals become exhausted [25]. This condition requires the prompt handling of these minerals to make a reasonable item. The most successive procedure of extricating zinc from poor quality zinc oxide stores is by the filter/dissolvable extraction/electrowinning process [26]. The utilization of entire metal filtering is probably not going to be financially savvy, and the detachment of corrosive consuming gangue minerals preceding draining is basic to the recuperation of zinc [19]. This has various benefits for filtering reagent use, treatment facility size, and site determination, since shipping zinc concentrate with high Zn grades could end up being financially reasonable. Using the buoyancy interaction, it is possible, in theory, removing upwards of 90% of the corrosive wasting gangue from ZnO metals and producing a concentrate with a zinc purity of 25-35 percent [27]. There have only been a few studies done on the buoyancy of zinc oxide metals, although buoyancy is the most common method used for the beneficiation and processing of oxidized zinc minerals [17]. The going with gangues of the chief zinc oxide mineral play a significant part in picking a reasonable buoyancy procedure [28,29]. Whole extraction process about zinc is given in figure 2.1.

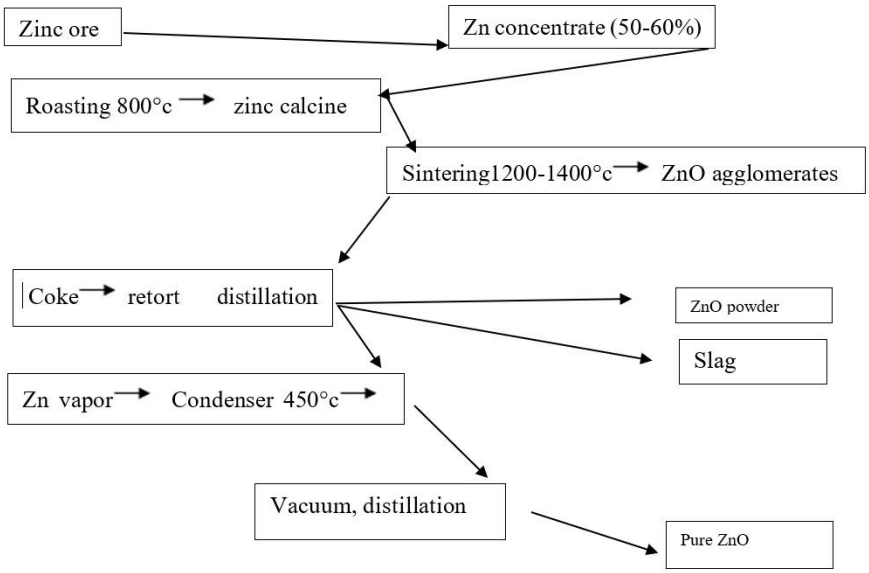


Figure 2.1. Extraction of Zinc Process [14].

## 2.3. ZINC BORATE

Zinc borate is a chemical compound with the formula $Zn_3(BO_3)_2$. It is a white powder that is widely used in a variety of industries due to its unique properties. In engineering, zinc borate is used primarily as a flame retardant, due to its ability to act as a synergist and a heat-sink. It is added to plastics, textiles, and other materials to slow down or prevent the spread of fire [28,30]. It is also used as a thermal stabilizer in engineering polymers, helping to prevent the thermal degradation of polymers and increases their thermal stability. Furthermore, it is also used as an additive in lubricants and lubricant additives, helping to improve the lubrication properties of lubricants and preventing the formation of deposits in the engine and transmission. In agriculture, it is used as a fungicide and insecticide, helping to protect crops from fungal and insect infestations [26].

Zinc borate is used as a flux for welding and brazing, and as a flux in the production of zinc coatings on steel and other metals in metallurgy and materials. It is also used as a desulfurizing agent in the production of high-quality steels. In ceramics, it is used as a flux and a refractory material, helping to lower the melting point of the ceramic mixture and improving the sintering properties of the ceramic [31]. Overall, zinc borate

is a versatile chemical compound that is used in a wide range of applications due to its flame-retardant, fungicide, insecticide, thermal stabilizer, lubricant additive, desulfurizing agent and refractory properties. It's chemical stability and non-toxicity make it a preferred choice for many industries [26].

It is impossible to find entity as the element boron existing by itself in nature; it can only be found in salts, where it is always referred to as borates and is defined as a combination that includes boric oxide. Boron can only be found in salts when it is combined with oxygen and other elements ($B_2O_3$) [26]. Borates are obtained in their whole from central region evaporites, which are the essential commercial sources of borates [32]. There are a limited number of nations with reserves rich in these minerals; the USA and Turkey, for example, provide 90% of the world's borate supply, but Turkey also has the world's largest reserves (borax, ulexite, and colemanite) [33]. The principal motivations behind borates and boron compounds are found in the finish and imaginative industry (sterile item, porcelain, earthenware, tiles), glass industry (diamonds, glass strands, heat proof Pyrex glasses, lights and spotlights), and fertilizers. Kernite is used to make boric destructive, tincal is used to convey sodium borate, and ulexite is used as the head fixing in the development of a combination of specialty glasses and earthenware production [34].

Hydrated and anhydrous metal borates are the two kinds of metal borates. Hydrated borates have B-OH packs in their plans and may consolidate interstitial water [35]. The plans of anhydrous metal borates are without water. Metal borates display an indispensable component of plastic product. Zinc borates, explicitly, are fabricated materials with expected applications considering their heat proof and smoke-retardant attributes [36]. Zinc borate compounds have the striking judiciousness of keeping its hydration water even at extraordinarily high temperatures. Considering its unprecedented warm strength, it's a renowned heat proof development for plastics and rubbers that require high taking care of temperatures, as well as an anticorrosive variety in coatings [37].

Boron is one of the seven major micronutrients that plants need; it may be administered directly to the soil, and it is also employed in the fertilizer type that is most well-known

[33]. It is accessible in the manufactured business (preparation of cleaning agents, color, fire retardants, abrasives, magnificence care items), tanneries (prevents rot), pharmacy (delicate sanitizer), and paints (fungicide) and is used as a wood added substance (considering its low harmfulness) and in capacitors, composites, versatile (fire retardant), and cement (moves back and helps to set) [31].

Industrially significant quantities of borate minerals are mined from both exogenous and endogenous borate sources. The former group consists of skarn-type and metamorphic borate deposits, whereas the latter group comprises volcanic-sedimentary and Salt Lake sedimentary borate or boron-rich brine [38]. The thermal breakdown of borates consists mostly of three processes: dehydrating crystal-water below 300 degrees Celsius, removing hydroxyl while the amorphous is present between 300 and 550 °C, and crystallization between 550 and 700 °C. The ulexite and tincalconite combine with calcite and magnesite, respectively, and then react at temperatures between 500 and 700 °C for two hours to form kotoite. This suggests that temperature, boron-rich fluid, and calcium-magnesium carbonate are the primary factors that control contact metamorphism [36,38]. Similar to skarn-type borate deposits, this gives a theoretical framework for the mineral combinations and wall rock modifications of metamorphic borate deposits. [38].

Zinc borate structures have been focused on actually as a result of their actual limit as driving forces and optical materials. Metal borates, in which boron is exclusively associated with oxygen, are abundant and comprehensively used in industry [39]. They may be found in both mineral and made structures. Various designed metal borates have a development that seems to be that of minerals, with single polyborate anions or frustrated polyborate rings, chains, sheets, or associations [39,40]. Structure sufficiency speculations spread out as of late for borate minerals, in any case, don't be guaranteed to apply to fabricated borates. Understanding how cations drive the essential units of borate compounds is fundamental for designed improvement [41]. Understanding how cations guide borate fundamental units in borate compounds is essential for making strong metal borates.

## 2.4. ZINC OXIDE

Zinc oxide is a white powder that is widely used in various fields due to its unique properties. It is an inorganic compound that is insoluble in water and has a high melting point. It is a wide bandgap semiconductor, which means it has a large energy gap between the valence and conduction bands, which leads to high electron mobility and high exciton binding energy, making it an attractive material for use in high-performance electronic devices such as transistors, solar cells, and light-emitting diodes [42]. Another important property of zinc oxide is its ability to absorb UV radiation, making it useful in sunscreens and other personal care products as well as in ceramics, glass, and other industrial applications. Additionally, it has low toxicity, making it a safe choice for use in biomedicine, medicine, and food products [43]. Zinc oxide also has a wide range of industrial applications, such as in ceramics and glass manufacturing, cement production, rubber, and plastics. It is also used as an ingredient in fire retardants, catalysts, and other chemical intermediates. Due to its combination of properties, zinc oxide is a versatile and useful material in various fields [9,44].

General properties and some crystal structures of zinc oxide mineral are given in table 2.1 and figure 2.2. Zinc oxide, which can be found in the periodic table's second and sixth groups, is an interesting material due to its many desirable qualities, such as its high electron mobility, broad band gap, and extreme simplicity, serious areas of strength for hole at room temperature, and so on. These properties are utilized in the arising utilizations of straightforward terminals in fluid precious stone presentations [45]. Because of its numerous modern applications, for example, electrophoresis, light-transmitting phosphor, shades in paints, glass-earthenware transition, elastic item fillers, paper coatings, sunscreens, drugs and beauty care products, ZnO has drawn in extraordinary interest in powder and slender film structure. and, surprisingly, its protection from radiation makes it valuable for space applications [46]. Research on ZnO nanostructures has been exceptionally well known in light of the fact that these materials can be utilized to make straightforward conductive oxides [47]. Since the shear modulus of the II-VI semiconductor is enormous, it doesn't insight as much execution debasement as other II-VI family semiconductors [48].

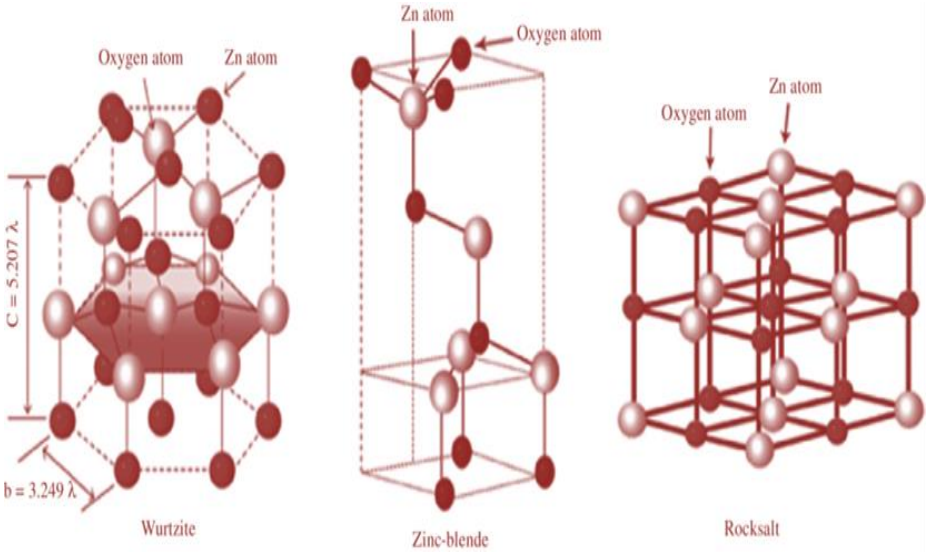


Figure 2.2. The Zinc Oxide Crystal structure of zinc blend-Wurzite-Rocksalt [49].

ZnO nanostructures may arise by nucleation and expansion. ZnO nanoparticle particles are shaped by inherent crystal characteristics during nucleation. ZnO Nano powders form hydrothermally as follows [27]. $Zn(NO_3)_26H_2O$, which is a precursor of basic zinc nitrate hexahydrate, hydrolyzes, resulting in the formation of zinc hydroxide ($Zn(OH)_2$) hydrosol [50].

Table 2.1. Proprieties of zinc oxide.

| No | Characteristics | Zinc Oxide | References |
|---|---|---|---|
| **1** | Another name | Zinc-white, Calamine, Zn-flower. | [51] |
| **2** | Formula | ZnO | [52] |
| **3** | Molar mass | 81.4 g/mol | [53] |
| **4** | Shape | Solid | [54] |
| **5** | Odor | No | [55] |
| **6** | Density | 5.6 $g/cm^3$ | [56] |
| **7** | Structure of crystal | Wurtzite | [57,58] |
| **8** | Geometry | Tetrahedral | [59] |
| **9** | Color | White | [60] |

# PART 3

# ENERGY DEPOSITION PROCESS

## 3.1. NANOPARTICLES SYNTHESIZE METHODS

Nanoparticles are tiny particles ranging in size from one to one hundred nanometers that differ from the bulk material due to their size. zinc, titanium, and silver are now used to create various metallic nanomaterials [10]. Nanoparticle combination might be finished in different ways, including physical, synthetic, and organic cycles. Physical and synthetic methodologies are for the most part remembered to be awesome for delivering consistently estimated nanoparticles with long haul dependability. These techniques, be that as it may, are exorbitant. Poisonous synthetic substances utilized in compound cycles for nanoparticle creation make the nanoparticles delivered less suitable [10,61].

Therefore, conventional theories and models fall short in their ability to describe the emergent traits when the dimensions are shrunk below 100 nm. Depending on their size, nanomaterials display better and unique features in comparison to huge particles of the same materials. The Earth naturally contains a vast variety of nanomaterials and particles, including photochemical byproducts, volcanic byproducts, and exhaust fumes. The development of stronger, better-quality, longer-lasting, more affordable, lighter, and smaller gadgets is the major goal of nanotechnology [62]. Numerous varieties of nanoscale manufacturing techniques are being created as a result. The section following goes into further information about them. The comment section also describe how nanoparticles that may be created for this purpose are used and characterized in supercapacitors [63]. There are two categories of nano - materials characteristics and generic nanomaterial properties in the area. While distinct kinds of nanomaterials display unique qualities, general features apply to all types of nanomaterials [64]. They may be synthesized using either bottom up or maybe even

a top-down method, and recent improvements have made it possible to have more control over their size, shape, and structure by choosing the right synthesis strategy and changing the synthesis conditions as seen in figure 3.1. Nanomaterials have many different electrical, physical, optical, and ferroelectric properties. capabilities, that have resulted in the discovery of several fascinating nanotechnology [65] the figure down shows the Top down approach and Bottom up approach for synthesis of Nanoparticles. At the same time, the visual regarding the classification of nano size described in the first chapter is given in figure 3.2.

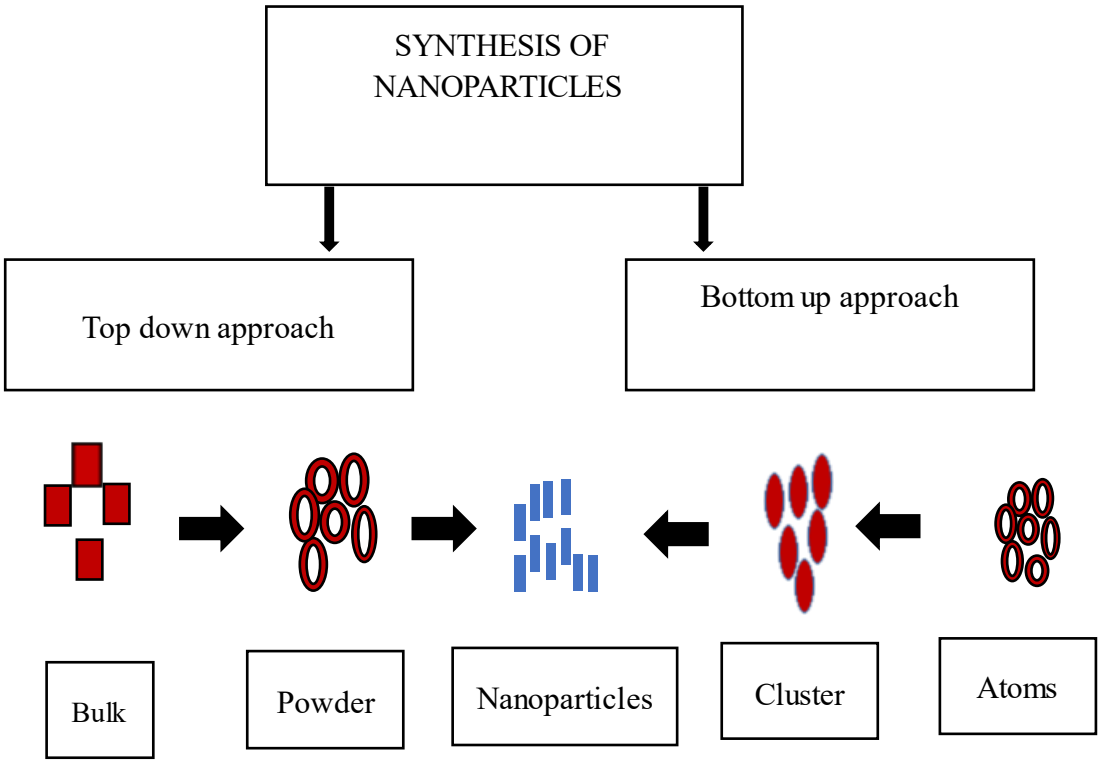


Figure 3.1. The top-down and bottom-up approach for making Nanoparticles.

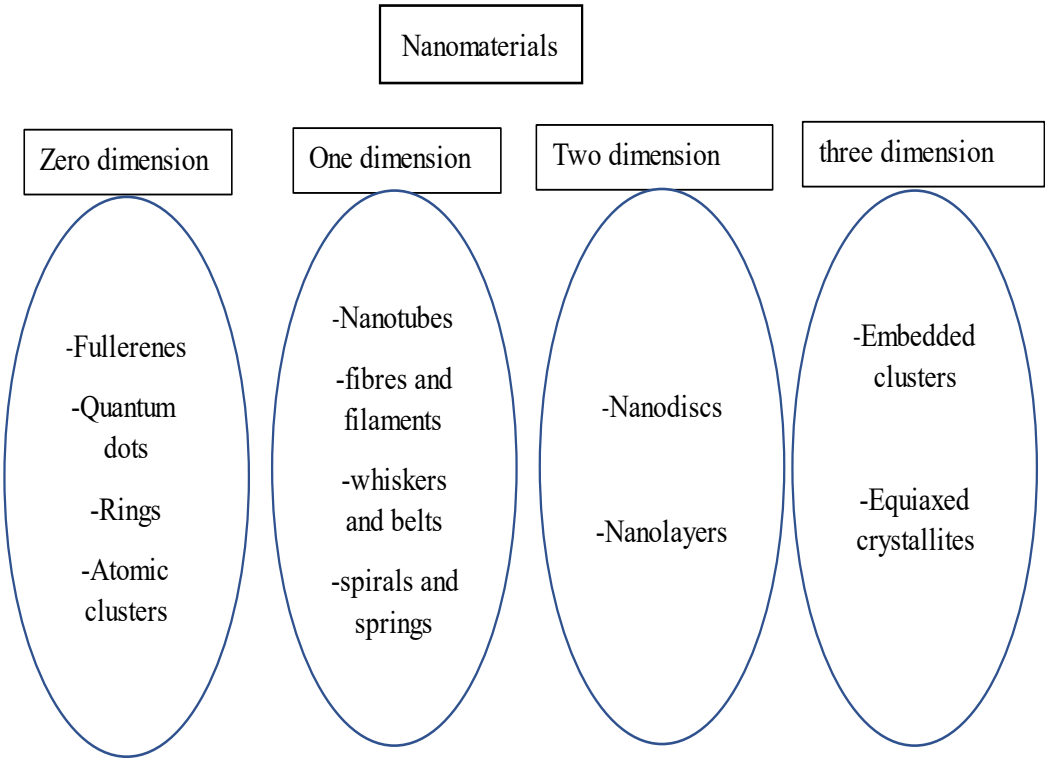


Figure 3.2. Classification-of-nanomaterials-on-the-basis-of-dimensions [66].

## 3.2. ENERGY STORAGE SYSTEMS

Energy storage systems (ESS) are systems that are designed to store and release energy as needed. They can be used for a variety of purposes, such as to smooth out the fluctuation of energy demand and supply, to provide backup power during power outages, and to support the integration of renewable energy sources into the grid [5]. There are several types of energy storage systems, including: Chemical storage systems, such as batteries, which store energy in the form of chemical energy and release it as electrical energy when needed as seen in figure 3.3 [67]. Thermal storage systems, such as molten salt storage, which store energy in the form of heat and release it as thermal energy when needed. Mechanical storage systems, such as pumped hydroelectric storage, which store energy in the form of potential energy and release it as kinetic energy when needed. Electrical storage systems, such as capacitors, which store energy in the form of an electrical field and release it quickly [67,68]. Each type of energy storage system has its own advantages and disadvantages and is suitable for different applications. The choice of an energy storage system depends on the specific requirements and constraints of a given application [69].

However, excessive ESS deployment is possible, which dramatically raises initial investment and maintenance expenses [70]. Energy storage technologies do not itself constitute energy sources, but they do provide significant advantages in terms of supply stability, power quality, and dependability. For power quality applications, advanced capacitors are being examined as a kind of energy storage. Although still in the testing phase, superconducting energy storage devices are getting attention for their potential utility applications. There include discussions of the most recent technological advancements, some performance analyses, and cost factors [67,70]. Another popular tool for storing energy as a surface charge that was created considerable period after batteries is the capacitor. This gadget requires a lot of surface area, which is directly related to how much energy can be stored and released from a capacitor with the smallest degree of damage to the components that make it up. Supercapacitors were created as a result of best attempts [67,69]. Energy capacity framework can chip away at the capability of energy networks in different ways. For example, they can free the stochastic individual from supportable power sources and work with their wide organization blend. Energy limit decisions may in like manner be utilized to work energy structures even more fiscally and cut down their running costs [69].

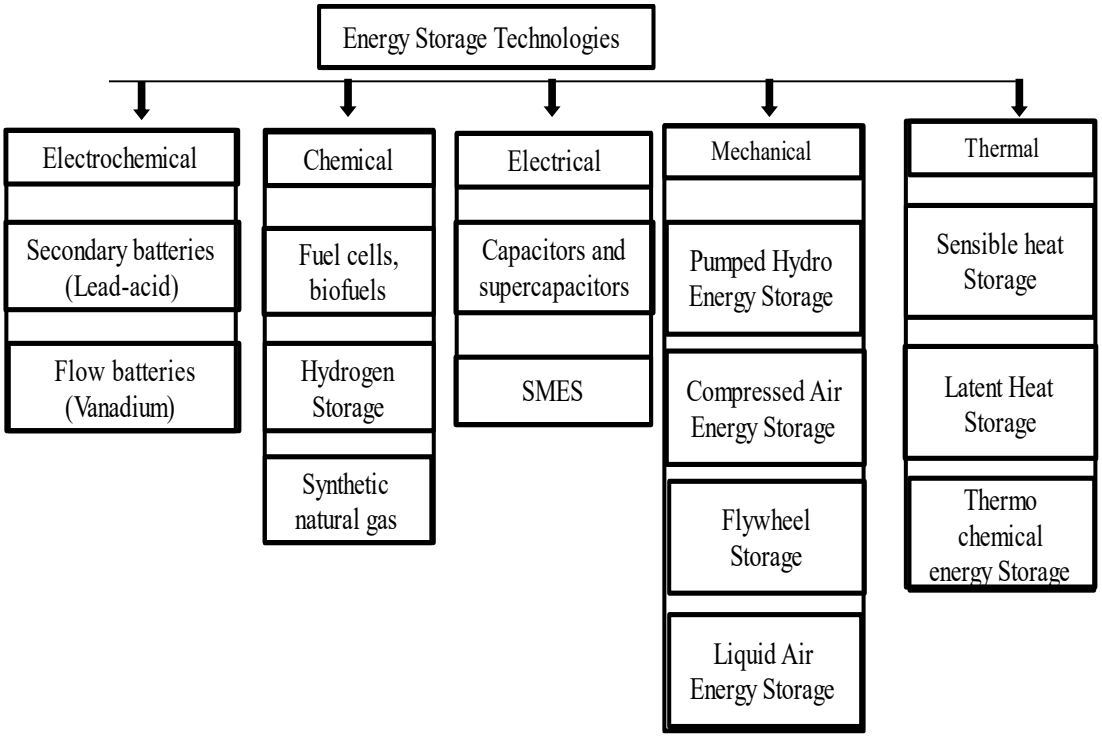


Figure 3.3. Classification of energy storage systems [68]

Utilizing ESS makes it commonsense to fortify the network during seasons of zenith load while taking care of energy at a limited expense during off-top hours, hindering sharp expense increases. Utilizing ESSs will similarly chip away at the efficiency of appropriated energy resources and addition supply/demand side controllability, which is useful for load changing or top shaving objectives [71]. To wrap things up, ESSs can offer repeat control organizations in places that are off the organization where there is an essential to stay aware of force balance under various working circumstances [67]. Each of the recently referenced uses for energy limit units has explicit execution essentials that ought to be meticulously considered during the arrangement connection and included into control and the board systems [70].

### 3.3. SUPERCAPACITORS

Supercapacitors, also known as ultracapacitors or electrochemical capacitors, are energy storage devices that are capable of storing and releasing large amounts of electrical energy very quickly [72]. They have much higher capacitance values than traditional capacitors, which allows them to store much more energy, and they have

several advantages such as high power density, long cycle life, wide operating temperature range, high safety and low maintenance, which makes them suitable for a wide range of applications such as power conditioning and power factor correction in electrical systems, energy smoothing in renewable energy systems, starting and stopping of engines in hybrid and electric vehicles, backup power supply in critical systems and powering electronic devices[3]. They are becoming increasingly popular in various fields due to their unique properties [73]. According to how they work, supercapacitors may be named either symmetric or asymmetric, on the other hand, ability due to the faradic (pseudocapacitive) participation between the terminal and the electrolyte [74]. Nevertheless, there are two unmistakable sorts of supercapacitor plans: sandwich supercapacitors, which have a vertical design with a separator sandwiched between two cathodes, and little supercapacitors (MSCs), which have an interdigital structure in comparable plane as the continuous finders and are disconnected from one another by a safeguarding opening (consistently of the solicitation for 10 to 100 s of micrometers) [75]. Finally, an electrolyte is placed on top of and between the cathodes to guarantee molecule transport along the terminals' basal plane [3].

However, electrochemical capacitors offer a far larger power capacity than batteries despite their lower energy density. Consequently, ECCs have qualities between those of regular capacitors and batteries, and they may compete with any or both of these types of components, depending on the nature of the task at hand [4]. In general, electrochemical capacitors (ECCs) may be a preferable choice over batteries in situations in which the quantity of energy to be stored is insufficient for a cell and the system's peak energy usage is disproportionately high in comparison to its typical power consumption [72]. When the energy storage requirements for a regular capacitor are met and the high-power pulse periods are not too short milliseconds or more, the ECC may be a viable alternative to traditional capacitors milliseconds or longer. The initial ECC devices had relatively modest power capabilities since they were intended to be used even as reserve of power for the purpose of storage restoration [73]. Beginning in the nineties, researchers have aimed to learn more about ECCs that can produce large amounts of electricity. High-power ECCs have decreased in price and increased in energy density steadily during the last 15 years [5,76]. Large markets for

ECCs have been predicted to emerge since the year 2000, and it is expected that within a few years, vast quantities of these devices would be commercially accessible for a variety of uses. Due to the due to expensive of big ECC devices, the industries for engine components, particularly those with capacitances of 1000 F or higher that compete with batteries, have expanded considerably more spontaneously than was anticipated. The markets for smaller devices, especially those with capacitances less than 1F, have grown rapidly [77].

## 3.4. CHARACTERIZATION OF SUPERCAPACITORS

Due to their high-power density and strong electrochemical performance, supercapacitors, a high energy-storage device with specific features, are suited for a wide range of applications. As a result, their industry has expanded quickly. Transportation, hybrid and electric cars, rail systems, and other applications might all benefit from the use of supercapacitors [77]. The need for energy and environmental pollution has intriguing answers in electric and hybrid automobiles. Supercapacitors are primarily used in industrial and household applications due to factors including environmental problems and special characteristics like high power density, minimal maintenance, straightforward operation, durability, and cost efficiency [74,77]. Currently, flexible and conductive fibers have garnered a lot of interest for supercapacitor devices due to the growing need for energy-storage devices with good electrochemical characteristics and the integration of electronic implements with textiles [78]. Supercapacitors have the potential for headway to be utilized as an eco-accommodating, non-volatile energy capacity hotspot for the eventual fate of wearable innovation since they consider extra scaling back prospects without compromising the high energy stockpiling limit and move rate [3].

The supercapacitor cathodes should have the accompanying qualities: an enormous surface region, long haul soundness, unbending nature to electrochemical oxidation or decrease, the capacity of different cycling materials, an ideal pore size conveyance, insignificant ohmic obstruction with the contacts, a palatable terminal electrolyte arrangement support association, underlying steadiness, and a low self-release level [77]. Charges on the surface and near the surface of such supercapacitors may be

saved by deposition and via pseudocapacitive processes that generate redox reactions on the surface. These are known as pseudo capacitors [79]. In electronic industry, industrial electricity and energy control, memory information storage, and it has thus been extensively used. It is employed in a variety of energy storage systems today, including those used in heavy machinery, electric cars, and portable electronics [80]. Supercapacitors are anticipated to have larger energy storage capacity and power density, as well as ultra-superior properties that can sustain lengthy cycles and have simple charge-discharge cycles, in particular for electric cars [81]. All criteria, not just one, should be created in order to achieve these requirements. For instance, it is necessary to enhance the characteristics of the collector material used as the electrode, such as increasing the energy density by being porous and having a larger surface area, while also using a dielectric material that can withstand long cycles and be charged-discharged quickly by performing simultaneous faradic reactions on this dielectric [82].

# PART 4

# LITERATURE REVIEW

## 4.1. SUMMARY OF PREVIOUS STUDIES

### 4.1.1. Leaching of zinc borate at different media

S. Gustu et al. carried out. leaching–purification–precipitation of zinc borates uses zinc ash. Zinc ash with Seventy-one percent zinc, six percent iron, twenty-eight percent chlorine, and two percent lead. and ppm levels of Cu, Cd, As, and others was solubilized in sulfuric acid. pH modification and borax ($Na_2B_4O_7 \cdot 10H_2O$) precipitation cleansed leach solutions. The phase compositions and shapes of precipitated zinc borates are hypersensitive to buffer pH, deposition temp, B-Zn mass ratio, or maturity duration. The zinc borate phase of interest ($3ZnO\text{-}3B_2O_3\text{-}3.5H_2O$) precipitated better at 95 °C and Ph 5.5–6.0 with B-Zn molar ratio >4.0.the Leaching–purification–precipitation has precipitated zinc borates from zinc ash [35].

Jiawei cheing. Carried out tests known as TCLP and M-PCT were used in order to look into the leachability of the FA30 glass. Based on the results of the TCLP test, it can be concluded that the heavy metals Pb, Zn, Ba, Cr, Cd, and Ni were effectively immobilized in the FA30 glass. According to the findings of the M-PCT tests, the ion-exchange process was the primary factor in the degradation of the glass. The breakdown of the glass structure in the FA30 glass led to the discharge of aluminum and iron into the environment. The breakdown of the glass structure might result in the discharge of heavy metals and could potentially affect the water sources [83].

Cihat tazioglu. carried out. zinc borate retention levels protected particleboards against degradation for 7 years but not termites. Particleboards used in southern Japan's climate need larger zinc borate loadings since Engagement as high as 2% (w/w) reduced infestation impact but did not fully protect. Wood-plastic composites were more resistant to fungus gnat degradation for 7 years, but in the final 18 months, even zinc borate embedded formulations had lower decay ratings. Zinc borate integrated formulations reduced termite destruction, however wood-polypropylene composites may need greater retentions for complete protection [84].

Ravina et al. carried out, integrating porphyrin derivatives with hydroxy phenyl groups into thin borate glass sheets for nonlinear semiconductor applications. Py (OH) 8 absorption and emission spectra redshift due to borate glass and -OH groups structural alteration. All molecules absorb intensity non-linearly. With increased input power, excitability saturation converts RSA to SA. RSA behavior relies on molecule hydroxy groups and excited state duration. -OH, groups increase electron concentration in excited states, lowering RSA effectiveness. This indicates optical commutators and ultrafast laser saturable absorbents [85]

Gaelle Fonain et al. investigated on neutralized intumescent fire retardant (NIFR) who has been successfully manufactured in "one step and one pot" utilizing a procedure that is straightforward, innovative, and risk-free. The conventional approaches to fire testing were used in order to assess the effectiveness of the NIFR in polypropylene (PP) as a fire suppressant. The findings indicate that the NIFR is a very efficient method. In addition to this, he demonstrated that zinc borate has a synergistic impact on the fire-retardant qualities of the material and that it seems to limit the migration of additives through the polymer matrix [30].

### 4.1.2. Zinc oxide production methods

Ka-lok Chui et al. decided to carry out the synthesis technique for the cheap manufacture of zinc oxide under air circumstances using a tiny polypropylene glass as a reactor Based on the findings of their XRD, FTR and SEM, TGA, and ultraviolet-visible (UV/Vis) investigations, these products were effectively achieved. Their

diameter is between 0.8 m and 2.6 m and their length is between 10 m and 40 m under optimal process settings, and their purity is higher than that of conventional ZnO powders. As-prepared ZnO microrods, on the contrary, have considerably lower photocatalytic performance, which means that are photostable and difficult to photodegrade polymers such as binders. As a consequence, they claim they will be a great and costly white powder with considerable possible covering uses [86].

Pooja Dasta et al. examined the use of biomass oil as a source of biodiesel and zinc, they found that Productivity and recycling, are better if the Zinc Oxide nanoparticles are doped with various transitions of metals. On the other hand, they prefer zinc oxides among all the heterogeneous Nano catalysts, because of their efficiency and their recyclability, which was obtained after having tested different oxides of various metals, and even to reduce the time and the temperature required for the synthesis of biodiesel [87].

Daitao Kuang et al. treated ZnO-doped ultra-small onion-type carbon nanoparticles (ZnO-OLC) with HCL, which resulted in the creation of OLC NPs. They discovered that ZnO-OLC NPs performed OLC NPs in terms of reflection loss (58.7 dB) and effective bandwidth (7.0 GHz) at 5% filler weight loading ratio. They indicated that by interacting with the atoms of Zn, O, and C, the dopant ZnO may lower the permittivity and loss of polarization of the OLC NPs, increasing their impedance adaption and micro-wave absorption [88].

Sen Yang et al. create a three-dimensional (3D) nanocomposite made out of Zinc oxide nanoparticles in the form of a flyer and 3D graphene (3DGZ). The morphological examination visualization indicated and the fact that perhaps the spaceship ZnO particles were evenly propagated and integrated in the three dimensional graphene that has not been amalgamated in any way, hence interesting for improving interfacial polarization, and that the 3DGZ-2 nanocomposites had the best microwave absorption, with a return loss of 48.05 dB measured around 11.71 GHz but then a layer of 1.82 mm, while RLs greater than 10 Because of their exceptional performance, 3DGZ nanocomposites have considerable potential as an efficient, lightweight, thermostable, and adjustable microwave absorber [89].

Xin Zheng et al. carry out the controlled co-precipitation production of additional nanomaterials and the use of without bender energetic materials and other materials. They prepared an Al-doped ZnO nanowire array using the hydrothermal method of CFI (continuous flow injection) to promote conductivity. This method was chosen appreciation to their offer of very stable concentration for doping which avoids the appearance of ZnO nanosheets with low conductivity, The increase in free moving electrons and holes greatly reduces the transfer resistance. The first basic approach has described the probable impact of Al doping. Based on this, Al-doped ZnO nanowire arrangements were produced as a binder-material [90].

### 4.1.3. Usage of zinc oxide in supercapacitors

Kulpriya Phetcharee et al. use carbon dots that have been bombarded with gamma rays and treated with amines to improve the efficiency of ZnO-based supercapacitors. Various doses of gamma radiation were applied to carbon spots in the presence of ethylenediamine (50-200). ZnO-CDs-EDA(50-200) electrodes' specific capacities boosted by 194% to 310%, from the comparison toward those of pure ZnO electrodes. It was discovered that somehow the changed carbon points in the electrodes improved not only the specific capacity, but also the controlled surface capacitance and series resistance, ion diffusion coefficient and electrochemical active area, electrode permeability and mechanical characteristics, and cycle stability after 8,500 cycles. This study demonstrates that ZnO-based supercapacitors may benefit from gamma-irradiated, amine-passivated carbon dots added to the electrodes, and that these carbon dots might be utilized to create supplemental high-capacity storage devices [91].

Gaurav Tatrari et al. study, spheres of graphene oxide (ZGS) generated from recycled tires that have undergone a process of fibrous reduction. Furthermore, the ZGS-based supercompensation device displays an exceptional power density of 3325 W kg-1 at a current density of 2 A g, as well as a fantastic energy density of 36,94 Wh Kg-1 at a current density of 2 Un g-1, all while possessing a high overpotential of 316,00 F g-1. from its electrochemical performance. Moreover, their primary classifications reveal a connection among symbiotic industries (SI), circular economy, and sustainable

development at a balayage speed of 5 m Vs-1 (DD). demonstrates very effective results for supercompensation [62].

Nidhi Tjwarj et al. Explored the possibility of a highly capacitive ZnCo2O4 electrode material being produced hydrothermally on a stainless-steel substrate. Microspheres of $ZnCo_2O_4$ were formed in a shape resembling broken nanosheets; the material has a specific capacity of 593 F/g at 10 mV/s and an internal resistance of 1.2 ; the zinc cobaltite electrode material has a columbic efficiency of 96.50%; and, by analyzing the data, the researchers concluded that zinc cobaltite microspheres are useful as effective super capacitive electrode materials with better specific capacity [62].

Sahana nayak et al Specifically, using zinc oxide and cobalt oxide nanocomposite, which has superior electrochemical capabilities and endurance, in a green synthesis. The morphology and electrochemical performance of the nanocomposite met with their approval. The power density of the synthesized nanocomposite electrode material is (3000-375.3) W/kg, and the energy density ranges from (3.8-9.54) Wh/kg. Energy densities range from (3.8-9.54) Wh/kg for the synthesized nanocomposite electrode material, while power densities range from (3000-375.3) W/kg throughout a wide range of current densities. With its many benefits over chemical processes, green synthesis is expected to become a practical technique for producing electrode components for energy storage devices that are used in cases utilizing alternative energy storing [62].

Tingting wei et al. carry out the zinc oxide nanoparticles' synthesis technique, reaction conditions, electrochemistry capabilities, and limits were examined, along with their present use in battery and hybrid supercapacitor (SC) technology. In particular, suggestions for improving the efficiency of zinc oxide-based materials are offered, along with forecasts for future research, development, practical applications, and industrialization of energy storage devices. And they come to the conclusion that Transition metal oxides (TMOs) may give a new route for the development of energy storage materials due to their exceptional stability, while also recommending the industrialization and practical applications of zinc oxides to boost the performance of zinc oxides-based materials [47].

Quanlu Wang et al. Investigated Polypyrrole (PPy) was polymerized on the surface of 1-dimensional columnar ZnCo-MOF utilizing $(NH_4)2S_2O_8/AgNO_3$ in the role of co-oxidant of PPy, and then ZnCo-MOF/PPy/$Ag_2O$ was obtained through in-situ oxidizing substance known as alizarin red S (ARS). They consider the PPy polymerization went well, and the electrode has a maximum capacitance due to the ARS's multifunctional effect as well as the oxidation that is catalyzed of ag to $Ag_2O$. The current density measured was 1 A/g [92].

Anuj KumarHis . Research on the sol-to-gel conversion induced by zinc acetate and polyethylene glycol to generate Zn alkoxide., with the aid of sodium hydroxide, led him to discover that calcination and drying led to the development of ZnO (NP) nanoparticles. Since the ZnO-AC nanocomposite was used as the electrode material to create the electrochemical double-layer tank cell (EDLC), and since 6 M KOH was used as the electrolyte, he performed TEM, SAED, and XRD analysis, and then studied the surface of the resulting nano-composites using scanning electron microscopy (SEM). Despite the high current and the little fluctuation in capacitance and density, he observed that the specific capacitance of the ZnO-AC (1:1) nano-composite was very high, at 118.122 mF $cm^2$. This suggests it might be used as an electrode material in supercapacitors [93].

Ü.Alver et al. Carry out for the supercapacitor electrode active materials, the researchers hydrothermally produced zinc oxide particles from zinc acetate, zinc chloride, and zinc nitrate (SC). They perform a 5 mV/s speed sweep in a 6 M KOH electrolyte and analyze the material using cyclic voltammetry, galvanostatic, and charge/discharge experiments, as well as X-ray diffraction, SEM and Raman spectroscopy to learn more about the material's electrochemical properties. Final ZnO electrode values for solutions of nitrate, acetate, and chloride are 5.87 F/g, 5.35 F/g, and 4.14 F/g, Approximately 5 F/g of capacitance was achieved when using the produced ZnO particles as electrodes in supercapacitors. Thus, ZnO particles synthesized from a nitrate precursor had better crystalline quality than those synthesized from an acetate precursor [94].

# PART 5

# EXPERIMENTAL PROCEDURE

## 5.1. MATERIALS AND METHODS

### 5.1.1. Raw materials

Zinc borate mineral purchased from Refsan was used to obtain zinc. Hydrochloric acid (HCl) with a concentration of 37% and pure water with a resistance of 18.25 Mohm were used in the extraction. Watman filter paper and centrifuge device were used in the filtration processes after extraction. The synthesis of nanoparticles from the extraction solution was carried out by hydrothermal method. For this purpose, stainless steel outer wall and Teflon lining were used. Nanoparticles were synthesized directly on the current collector nickel foam surface. Karabuk University Materials Research and Development Laboratories were used for all other laboratory equipment such as ovens, precision scales and scales.

Figure 5.1. Zinc borate used in experiments.

For attempting to describe the products obtained from the hydrothermal method of producing metal oxide on the nickel foam, crystallographic evaluation was carried using the Rigaku Ultima IV X-ray diffraction (XRD) equipment. These evaluations made use of Cu-based Ka radiation (=0.1546 nm) produced by a stable monochromator running at 40 kV and 40 mA, with a 2-frequency varying from 10-80°. In order to characterize the chemical bonds in these substances, we next employed a Bruker Alpha brand Fourier transform infrared spectrometer in order to transmit data to perform studies between 400 and 4000 $cm^{-1}$ wave number with $2cm^{-1}$ precision (FTIR). Microstructure and morphology were also examined by looking at pictures taken with a Carl Zeiss ULTRA PLUS Scanning Electron Microscope (SEM). The instruments in use for this initiative are shown in figures 5.2, figure 5.3, and figure 5.4.


Figure 5.2. X-ray diffraction instrument (XRD)


Figure 5.3. Fourier transform infrared spectroscopy (FTIR).


Figure 5.4. Scanning electron microscope (SEM).

### 5.1.2. Workflow chart

Zinc oxide in solutions during zinc borate extraction is essential for such experiments. That although abovementioned elements are usually sought in metallic form, metal oxides are required in specific sectors. Nanosized metal oxide production on a metal collector surface layer improves energy storage performance in supercapacitors. This work aims to synthesis zinc oxide-based metal oxide nanoparticles from the solution with the maximum zinc oxide extraction from zinc borate, It is expected to use the nanoparticles supercapacitors to be produced at this step to hold electricity power at the anode electrode. With this fundamental reason, it must be produced on a conductive layer. Nickel foam, with a huge surface area, is a preferred supercapacitor conductive layer. This work synthesizes zinc oxide-on-nickel foam metal oxide nanoparticles. The hydrothermal technique is some of the most useful manners that may offer nanoparticle synthesis in a liquid environment and on a metal surface. It is also one of the most often used methods. Before beginning production using this approach, the solution that had the greatest concentration after the previous step was identified first. This was performed in order that the production could begin. After that, 7 ml of this solution were transferred into an autoclave made of stainless steel and Teflon that had a capacity of 40 ml. This autoclave also received two pieces of nickel foam measuring 0.5 by 3 centimeters that had been cut to the same size during the same time. After that, the lid of the Teflon liner was secured, and then the lid of the autoclave made of stainless steel was secured as well. The same technique was carried out in the other 3 autoclaves, bringing the total number of autoclaves that were used in the manufacturing to 4 again after, the autoclaves were put into the furnace and warmed to a temperature of 120 ° C. before being left there for a period of six hours. Following the completion of this procedure, the autoclaves were taken out of the oven and allowed to return to their normal temperature. After that, the lids were unlocked, and the nickel foams are removed before being rinsed in deionized water to eliminate any residues that may have been on them. After that, it must have been dried at a temperature of sixty degrees Celsius for twenty-four hours and then exposed to dehumidification. In addition, because the solutions in the autoclave also include particles of the produced product and may be used in the procedures of analysis, they were transferred into glass tubes and centrifuged at a speed of 3000 rpm for 15 minutes.

After that, the liquid that was left over was emptied off, and the particles that were left as deposit were in the oven to dry for one day. Therefore, nickel foam processing and production were performed up.

### 5.1.3. Leaching and its characterization processes

In this section of the research, the procedures for producing solutions with varying parameters in order to separate zinc oxide components from zinc borate. To achieve this objective, firstly, a beaker with a capacity of 250 ml was obtained, and then 50 ml of deionized water was introduced into it. Next, the beaker that contained this combination was putted on the heater, and magnetic stirring was continued until the temperature reached 80 °C. When the temperature hit 80 °C, three grams of zinc borate were weighed into the beaker and added to the mixture. At the same temperature, the stirring was carried on for an hour. These procedures were performed in the configurations shown in Table.5.1.

Table 5.2. Extraction of Zinc from Zinc Borate Parameters.

| HCl | Water | Zinc borate | Time | Stirring | Temperature |
|---|---|---|---|---|---|
| 0 | 50 ml | 3 grams | 60 min. | 360 rpm | 80 °C |
| 1 | 50 ml | 3 grams | 60 min. | 360 rpm | 80 °C |
| 3 | 50 ml | 3 grams | 60 min. | 360 rpm | 80 °C |
| 5 | 50 ml | 3 grams | 60 min. | 360 rpm | 80 °C |
| 7 | 50 ml | 3 grams | 60 min. | 360 rpm | 80 °C |
| 9 | 50 ml | 3 grams | 60 min. | 360 rpm | 80 °C |

The mixture was poured into a beaker, filtered through a funnel and paper to filter the solution. The figure 5.5. shows the process.

Figure 5.5. Extraction preparation and filtration.

On the other hand, we use ammonium ($NH_4HF$), distilled water, urea and zinc chloride with sintering  at 110 rpm the table down shows the details.

Table 5.3. Hydrothermal Prepation Parameters

| zinc chloride | Ammonium | Urea | Distilled water | sintering | Time |
|---|---|---|---|---|---|
| 10 mg | 10 mg | 20 mg | 5 ml | 110 rpm | 15 min. |
| 70 mg | 10 mg | 20 mg | 5 ml | 110 rpm | 15 min. |
| 150 mg | 10 mg | 20 mg | 5 ml | 110 rpm | 15 min. |
| 250 mg | 10 mg | 20 mg | 5 ml | 110 rpm | 15 min. |

### 5.1.4. Zinc oxide production and characterization

The zinc oxide concentrations of the solutions  produced during extraction was evaluated by Thermo Scientific Ice 3400 atomic absorption spectrometers (AAS). A dilution into stock solutions was the first step in the beginning of this procedure. Because the zinc oxide concentrations in the stock solutions are higher than the AAS measurement limit, the reason for this dilution is so that they may be measured, in this procedure, 500 microliters of stock solutions were drawn out and combined with 50

milliliters of deionized water to produce measurement preparations with a concentration of 5 M. These collections were known as diluted solutions. On the other side, additional preparations of 1 ppm, 3 ppm, and 5 ppm were made independently from 1000 ppm zinc standard solutions by employing the same dilution method and were used for the measurement. Those preparations were known as calibration solutions. The device's flame measurement function and zinc cathode tubes were used to get the measured values. In the beginning, the zinc tube was activated, and then it was left unattended for around 15 minutes to stabilize. First, a procedure was developed in which calibration solutions were used for the first three tests, followed by more dilute samples. This approach was used to begin the measurements, and the first thing that was done was to measure the concentrations of standard solutions with strengths of 1 ppm, 3 ppm and 5 ppm. It was indicated that it should yield 0.4 absorbance at 1 ppm concentration according to the results in the flame measuring test of the zinc in the software, and the measured values of the standard solutions were achieved in this direction. After that, the procedure was finished off by analyzing the diluted samples of the test. even after extraction, all of the stock solutions were weighed in the same manner. Figure 5.6 and the figure 5.7. shows the solutions made by the AAS device that was used for this study.

Figure 5.6. Extraction solutions.


Figure 5.7.  Atomic absorption spectroscopy (AAS).

### 5.1.5. Preparation and characterization of supercapacitor electrodes

The electrochemical performance of metal oxides generated hydrothermally directly on nickel foam surface was investigated at room temperature using a potentiometer of the Parstat 4000. A three-electrode test device was used for this research. Graphite was used as the counter electrode, Ag/AgCl served as the reference electrode, and metal oxide doped nickel foam served as the working electrode, as illustrated in figure 5.8. Measurements were made in a 6M KOH solution. This solution was created using deionized water that is 18.25 Mohm resistant. Prior to the measurements, a force of roughly 10 MPa was applied to the nickel foam to flatten it. The KOH solution-filled beaker was then filled with the electrodes. The working electrode, a 1 $cm^2$ patch of nickel foam, was positioned such that it was immersed in this mixture. Immediately after the end of this procedure, galvanostatic charge discharge measurements were carried out utilizing the Versa studio software application within the range of 1-6 mA. It was possible to calculate the discharge times at each current density based on all these data. After that, measurements for the particular areal capacitance, represented by the symbol Cs, was determined by using the formula found in equation 5.1 :

$$C_s = I \times \Delta t / \Delta V \times s \tag{5.1}$$

The value of Cs in this formula represents the area capacitance in millifarads (mF), I represents the discharge existing constant in milliamperes (mA), t represents the discharge time in seconds, V represents the potential window in volts, and S represents the surface area of the working electrode in cm2. Also, using this information, we were able to compute the electrode's energy (E) and power (P) densities using equations 5.2 and 5.3.

$$E = Cs \times V^2/7.2 \tag{5.2}$$

$$P = 3600 \times E / \Delta t \tag{5.3}$$

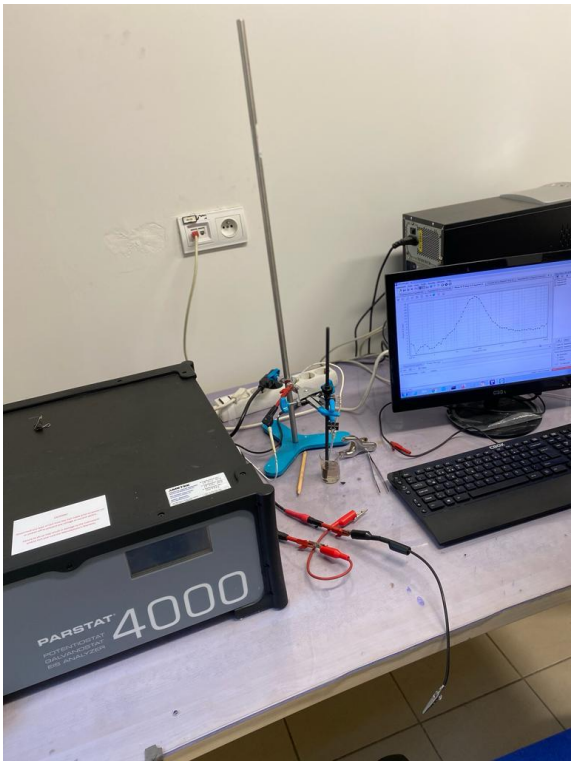


Figure 5.8. Electrochemical measurement device.

# PART 6

# RESULTS AND DISCUSSION

## 6.1. ZINC CONCENTRATIONS OF LEACHING SOLUTION

Zinc borate mineral was used as a source for the synthesis of zinc oxide synthesis nanoparticles in this study. For the extraction of zinc metal from this mineral, hydrochloric acid treatment was carried out at different concentrations. For this purpose, 6 different solutions with acid concentrations of 0 ppm, 20 ppm, 60 ppm, 100 ppm, and 140 ppm were prepared. Further details of solution preparation and extraction were described in the procedure section. Here, the zinc metal concentration of each solution measured by AAS is given in the graph in figure 6.1. According to these results, it was observed that the zinc concentration of the solution with no acid was 5.1 ppm, while that of the 20-ppm acidic solution was 108 ppm. On the other hand, when the acid concentration was increased to 60 ppm and 100 ppm, zinc concentrations increased to about 130 ppm for both of them. There is a fairly linear increase here. However, when the amount of acid was increased to 7 ppm, the zinc concentration reached its maximum with 127 ppm. When more acid was added than this, the zinc concentration became saturated and changed by almost negligible amounts. This stabilization was probably due to the fact that the mineral source remained constant, and the maximum amount of zinc was extracted from the mineral, despite the increase in chlorine ions from the acid in the solution.

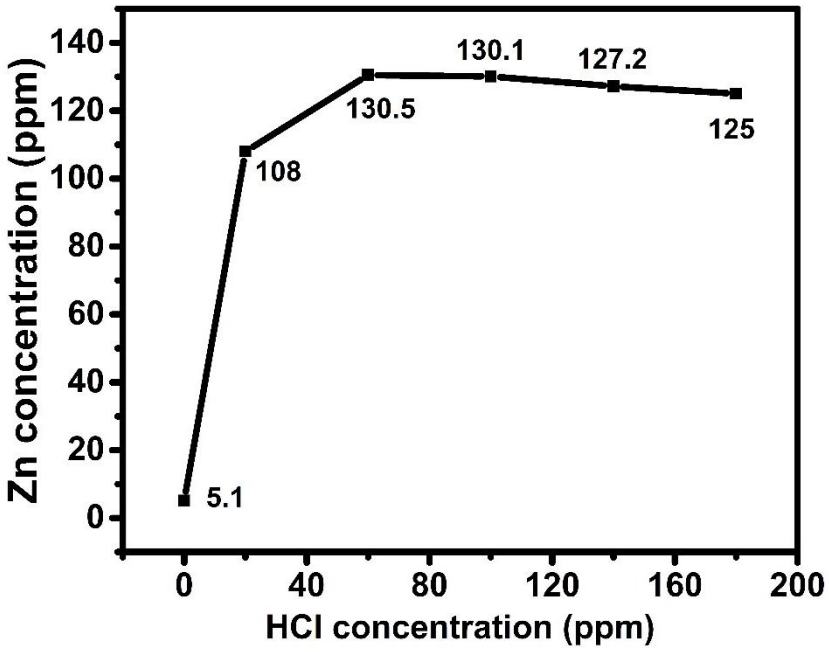


Figure 6.1. Zinc concentrations measurement by AAS.

## 6.2. CHARACTARIZATION OF PRODUCED ZINC OXIDE

Characterization studies were first started with X-ray diffraction pattern analysis. In this analysis, firstly the raw material, zinc borate, then the semi-finished product after extraction and finally the post-synthesis products by hydrothermal method were analyzed. The results are given in figure 6.2. According to these results, the 2θ value of the raw material zinc borate gave characteristic peaks between about 15° and 70° (JCPDS File No. 35-0433) [95]. In the semi-finished product, two sharp peaks were observed at approximately 25° and 28°, which are highly compatible with the characteristic zinc chloride planes of (112) and (103), respectively [96]. Finally, peaks of the (100), (002) and (101) planes were observed at approximately 31°, 34° and 36°, respectively, indicating zinc oxide [97]. Apart from these, additional peaks were also observed in the final product, which indicates that some $ZnCl_2$ compound remained in the structure. In Figure 6.2, FTIR analysis results for interatomic bond characterization are given. In this chart, the same analyzes were performed in XRD. The characteristic B3-O, B-O-H and B4O bonds of the raw material zinc borate were observed. In the semi-product, there are observations of O-H bond and C-O bonds. These are due to

possible impurities and moisture in the sample. Zn-O was observed in the final product, which indicates the formation of zinc oxide. However, the low strength of the Zn-O bond is probably due to the strength of other impurities [95].

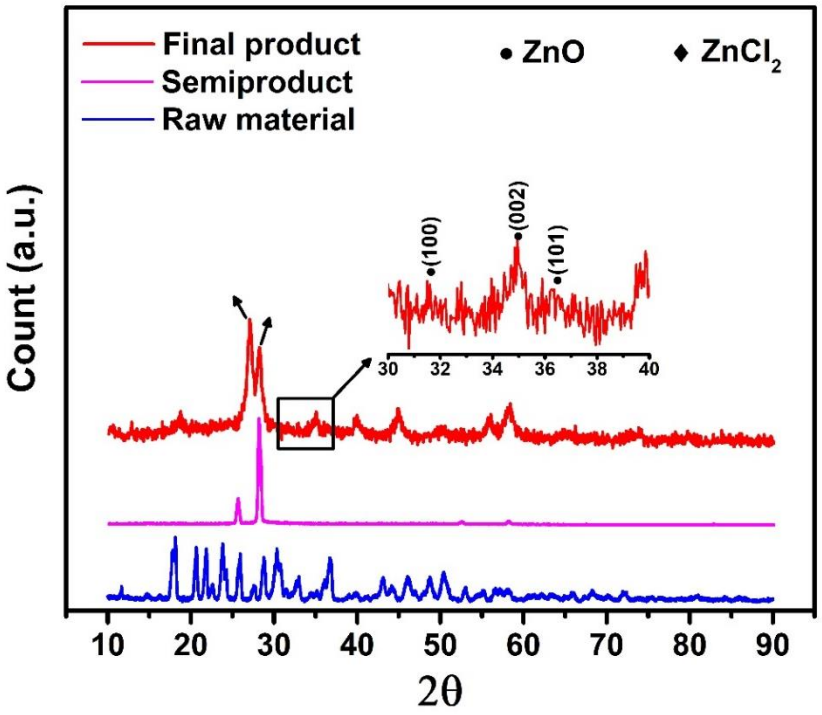


Figure 6.2. XRD result of synthesized zinc oxide and others

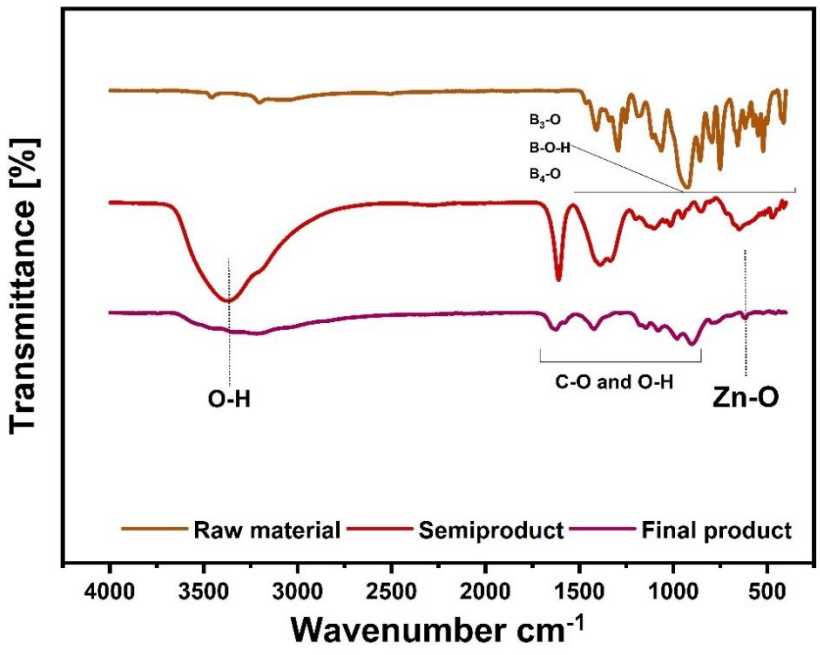


Figure 6.3. FTIR result of synthesized zinc oxide and others.

The geometric structure of the formations on the nickel foam surface of the products after hydrothermal production was examined with a scanning electron microscope as seen in figure 6.4. According to these results, there are rod-shaped and strip-shaped formations on the surface of pure nickel foam. These formations are understood in the general views in figures 6.4a and b. In the view in Figure 6.4c, it is understood that these formations have a strip-like geometry rather than a bar. The dimensional distribution of these strips was measured with the Image J software program and plotted with origin and graphed as in figure 6.4 d. This graph shows that the average size is around 358 nm. It can also be said that less than 10% of these bars are around 100 nm. It has been widely stated in the literature that zinc oxide crystals are synthesized in rod-like form. However, the fact that it was synthesized in strip form in this study provides an important originality [98,99]. On the other hand, it has been said in the literature that such nano-sized formations increase the surface area of the current collector (nickel foam) to increase its capacity to hold more ions, and thus its electrochemical performance is improved [100,101]. Based on this information, it was characterized that a large surface area supercapacitor electrode in the form of a strip was synthesized from zinc borate mineral in a clean way.

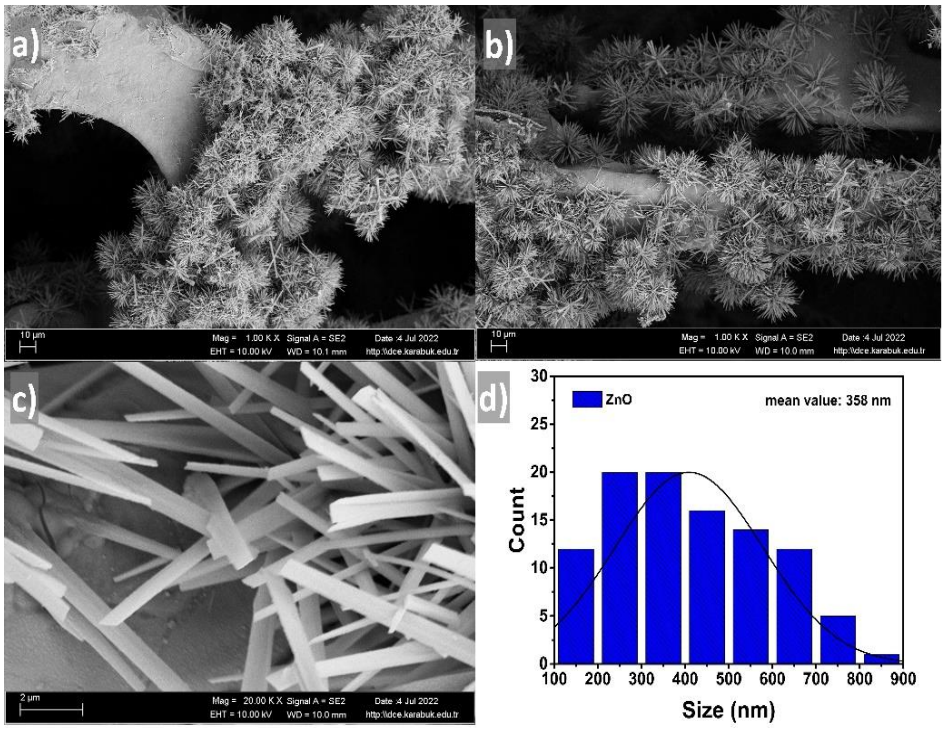


Figure 6.4. a-b-c) images of synthesized zinc oxide nanorods in different growth d) distribution histogram plot of nanorods.

## 6.3. ELECTROCHEMICAL RESULTS OF ZINC OXIDE ELECTRODES

Electrochemical performances of zinc oxide nanorods synthesized on nickel foam surface by hydrothermal method are investigated in this section. For this purpose, firstly, cyclic voltammetry and then galvanostatic charge-discharge measurements were carried out. The measurement results obtained are given in figure 6.5 and figure 6.6. As can be seen from these graphs, the measurements were carried out at different scanning speeds. According to these results, it was observed that faradic redox reactions occurred in the anodic and cathodic regions, possibly due to M-O and M-OH (M: Zn) bonding [97]. The intensity of these peaks increased and decreased proportionally with the scanning speed [102]. This ratio shows that redox reactions occur reversibly. The increase/decrease of their intensity is related to the faster or slower attraction of the ions in the solution to the electrodes depending on the applied potential [103,104].

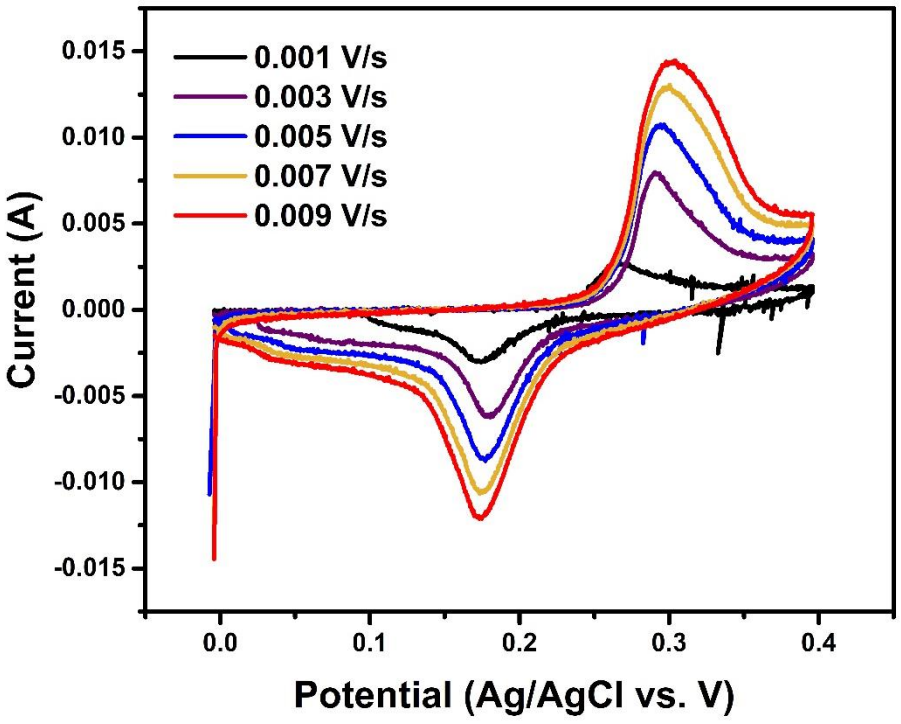


Figure 6.5. Cyclic voltammetry measurement results.

In order to measure the performance of the electrode, galvanostatic charge-discharge measurement was carried out. This measurement was also performed at different current densities, similar to the CV. The results are given in figure 6.6. According to these results, it can be said that the electrode has a battery type charge cycle. Secondly, it was observed that the discharge time decreased as the current density increased. This is related to the rapid influx of ions in solution at high currents to the electrode surface and possibly forming an ion layer on the surface. It can be said that this ion layer formation prevents ions from entering the inner parts of the electrode and therefore reduces the discharge time. This situation has been similarly explained in the literature [105]. On the other hand, discharge times from 1 mA to 6 mA were observed to be 212 s, 76 s, 43 s, 32 s, 25 s, and 19 s, respectively. The specific capacitance values related to these times were calculated as 557 mF/cm$^2$, 400 mF/cm$^2$, 339 mF/cm$^2$, 336 mF/cm$^2$, 328 mF/cm$^2$, and 300 mF/cm$^2$, respectively, according to the formula in equation 5.1. The changes in the specific capacitance values depending on the current density are given graphically in figure 6.7. As can be seen from the graph, the specific capacitance decreased as the current density increased. The reason for this is related to the fact that the ions do not have time to enter the inner parts of the electrode and accumulate on the surface with high current, as stated above.

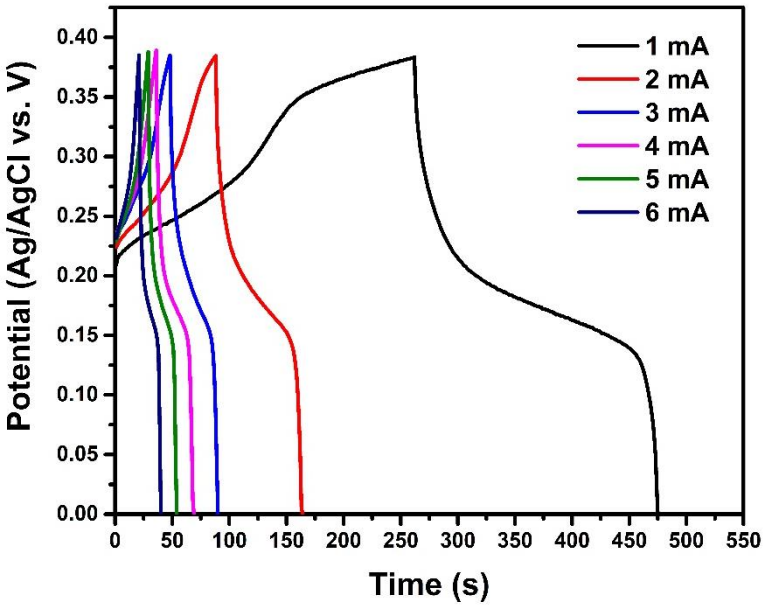


Figure 0.6. Galvanostatic charge – discharge measurement results.

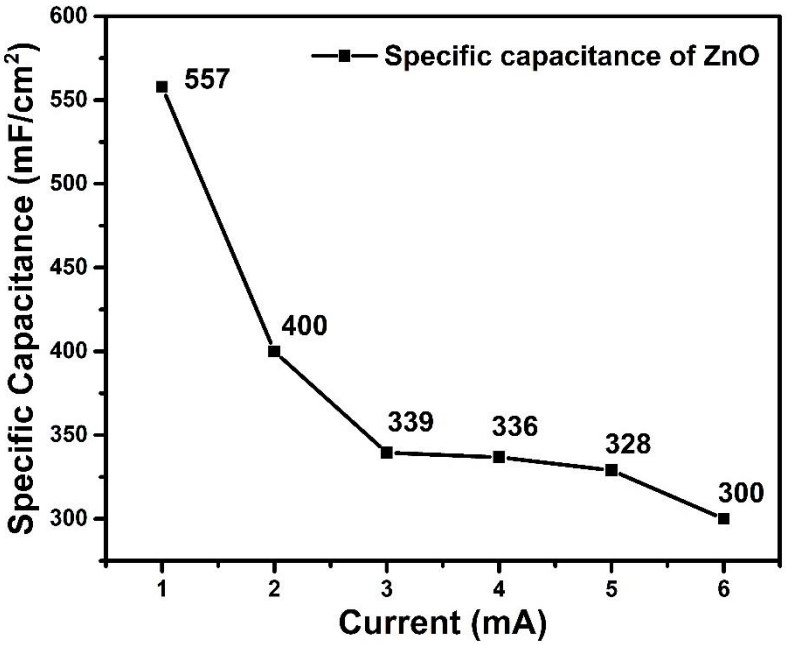


Figure 6.7. Specific capacitance calculation results.

The specific capacitance value of the electrode is directly related to the amount of energy and power storage. The formulas given in Equations 5.2 and 5.3 are widely used to calculate these values. In this study, using the aforementioned formulas, the energy and power densities of the electrode were calculated and given in the graph in figure 6.8. According to these results, the highest energy density was calculated as approximately 11.2 mWh/cm$^2$ at 1 mA and the power density was calculated as approximately 200 mW/cm$^2$. It was observed that the energy density decreased as the current value increased. This decrease probably means that the electrode holds fewer ions. On the other hand, the lowest value of energy density and the highest values of power density were obtained as 6 mWh/cm2 and 1140 mW/cm2, respectively, at 6 mA current.

In the literature, it has been reported that the energy density is related to the large surface area of the particles forming the electrode, while the power density is related to the redox reactions occurring on the surface. While the surface area of the electrode increases with nano-sized syntheses, it is known that redox reactions are related to the formation of metal oxides that can give reduction and oxidation of these surfaces [105–107]. The zinc oxide rods synthesized in this study with an average thickness of

approximately 350 nm meet both of the aforementioned precursors. For this reason, the fact that the produced electrode reaches a specific capacitance of almost 550 mF/cm$^2$ without any other contribution also confirms this. The specific capacitances of many equivalents of zinc oxide in the literature are well below 550 mF/cm$^2$ [97,108]. However, the energy density at this level is quite low. It is very promising to achieve high-level performances by decorating the zinc oxide electrode, which performs at this level alone, with another component [109,110].

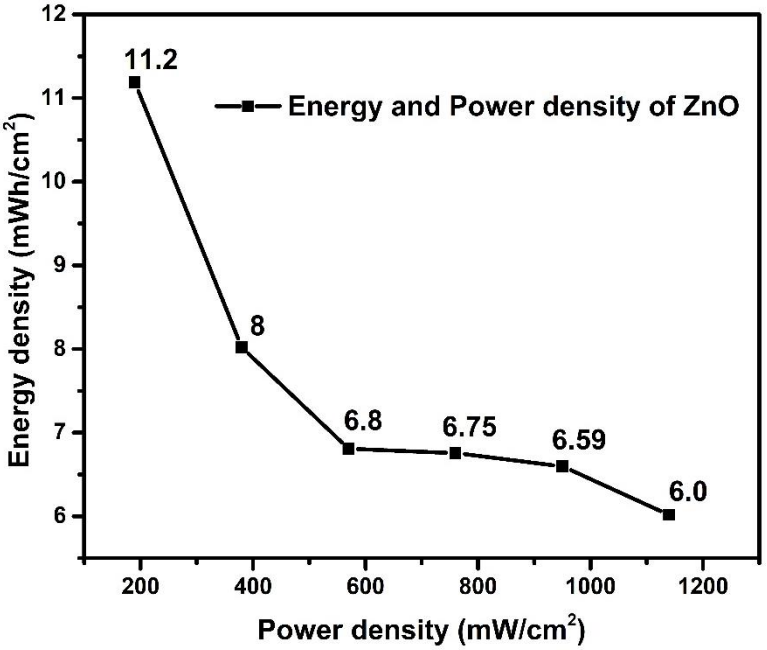


Figure 6.8. Energy and power density calculation results.

.

# PART 7

## SUMMARY

This study aims to produce a supercapacitor electrode based on the mineral. For this purpose, firstly, zinc metal extraction was carried out with hydrochloric acid from the zinc borate mineral. Extraction results showed that the highest zinc concentration was obtained at approximately 130 ppm in 60 ppm HCl solution. In addition, it was observed that the zinc concentration reached saturation level at acid concentrations above 60 ppm, and no further increase occurred. The highest concentration solution was used for zinc oxide metal synthesis. The hydrothermal method carried out the synthesis directly on the nickel foam surface. The product obtained here was first characterized by XRD, FTIR, and SEM analyses. The characterization results confirmed that the products consisted of an average of 358 nm zinc oxide nanorods. Electrochemical results showed that the electrode has a battery-type charging mechanism, and the highest specific capacitance is 557 $mF/cm^2$ at a current density of 1 $mA/cm^2$. It also showed that this electrode's energy and power density values were 11.2 $mWh/cm^2$ and 200 $mW/cm^2$, respectively, at a current density of 1 $mA/cm^2$.

## REFERENCES


1. Wang, H., Liang, Y., Mirfakhrai, T., Chen, Z., Casalongue, H. S., and Dai, H., "Advanced asymmetrical supercapacitors based on graphene hybrid materials", ***Nano Research***, 4 (8): 729–736 (2011).

2. Khairy, M., El-Shaarawy, M. G., and Mousa, M. A., "Characterization and super-capacitive properties of nanocrystalline copper ferrite prepared via green and chemical methods", ***Materials Science And Engineering: B***, 263: 114812 (2021).

3. Polat, S., "Production of ZnFe2O4 Doped Carbon Cloth-Based Flexible Composite Electrodes for Supercapacitors", Türk Doğa Ve Fen Dergisi, 10 (2): 199–205 (2021).

4. Polat, S., "Dielectric Properties of GNPs@MgO/CuO@PVDF Composite Films", Erciyes Üniversitesi Fen Bilimleri Enstitüsü Fen Bilimleri Dergisi, 37 (3): 412–422 (2021).

5. Xiao, J.-W., Yang, Y.-B., Cui, S., and Liu, X.-K., "A new energy storage sharing framework with regard to both storage capacity and power capacity", ***Applied Energy***, 307: 118171 (2022).

6. Rani, N., Saini, M., Yadav, S., Gupta, K., Saini, K., and Khanuja, M., "High performance super-capacitor based on rod shaped ZnO nanostructure electrode", ***AIP Conference Proceedings***, 2276 (1): 020042 (2020).

7. Chairaksa-Fujimoto, R., Maruyama, K., Miki, T., and Nagasaka, T., "The selective alkaline leaching of zinc oxide from Electric Arc Furnace dust pre-treated with calcium oxide", ***Hydrometallurgy***, 159: 120–125 (2016).

8. Verma, R. K., Nagar, V., Aseri, V., Mavry, B., Pandit, P. P., Chopade, R. L., Singh, A., Singh, A., Yadav, V. K., Pandey, K., and Sankhla, M. S., "Zinc oxide (ZnO) nanoparticles: Synthesis properties and their forensic applications in latent fingerprints development", ***Materials Today: Proceedings***, 69: 36–41 (2022).

9. Moezzi, A., McDonagh, A. M., and Cortie, M. B., "Zinc oxide particles: Synthesis, properties and applications", ***Chemical Engineering Journal***, 185–186: 1–22 (2012).

10. Begum, S., Karim, A. N. M., Ansari, M. N. M., and Hashmi, M. S. J., "Nanomaterials", Encyclopedia of Renewable and Sustainable Materials, ***Elsevier***, Oxford, 515–539 (2020).

11. Polat, S., "Dielectric Properties of BN-ZnO-GNP Doped PU-EG Composites", International Journal Of Engineering Research And Development, 13 (2): 635–644 (2021).

12. Khan, I., Saeed, K., and Khan, I., "Nanoparticles: Properties, applications and toxicities", ***Arabian Journal Of Chemistry***, 12 (7): 908–931 (2019).

13. Yudaev, P. A., Kolpinskaya, N. A., and Chistyakov, E. M., "Organophosphorous extractants for metals", ***Hydrometallurgy***, 201: 105558 (2021).

14. Kashyap, V., Taylor, P., Tshijik Karumb, E., and Cheshire, M., "Application of zinc ferrite reduction in the extraction of Zn, Ga and In from zinc refinery residue", ***Minerals Engineering***, 171: 107078 (2021).

15. Mudd, G. M., Jowitt, S. M., and Werner, T. T., "The world's lead-zinc mineral resources: Scarcity, data, issues and opportunities", ***Ore Geology Reviews***, 80: 1160–1190 (2017).

16. Wang, D., Liang, Y., Lin, Z., Peng, C., and Peng, B., "Comprehensive recovery of zinc, iron and copper from copper slag by co-roasting with SO2–O2", ***Journal Of Materials Research And Technology***, 19: 2546–2555 (2022).

17. Trpčevská, J., Hoľková, B., Briančin, J., Korálová, K., and Pirošková, J., "The pyrometallurgical recovery of zinc from the coarse-grained fraction of zinc ash by centrifugal force", ***International Journal Of Mineral Processing***, 143: 25–33 (2015).

18. Ke, Y., Peng, N., Xue, K., Min, X., Chai, L., Pan, Q., Liang, Y., Xiao, R., Wang, Y., Tang, C., and Liu, H., "Sulfidation behavior and mechanism of zinc silicate roasted with pyrite", ***Applied Surface Science***, 435: 1011–1019 (2018).

19. Li, Y.-C., Min, X.-B., Chai, L.-Y., Shi, M.-Q., Tang, C.-J., Wang, Q.-W., Liang, Y., Lei, J., and Liyang, W.-J., "Co-treatment of gypsum sludge and Pb/Zn smelting slag for the solidification of sludge containing arsenic and

heavy metals", ***Journal Of Environmental Management***, 181: 756–761 (2016).

20. Schippers, A., Tanne, C., Stummeyer, J., and Graupner, T., "Sphalerite bioleaching comparison in shake flasks and percolators", ***Minerals Engineering***, 132: 251–257 (2019).

21. Ke, Y., Peng, N., Xue, K., Min, X., Chai, L., Pan, Q., Liang, Y., Xiao, R., Wang, Y., Tang, C., and Liu, H., "Sulfidation behavior and mechanism of zinc silicate roasted with pyrite", Applied Surface Science, 435: 1011–1019 (2018).

22. Feng, Z., Liu, G., Li, Y., Zhu, H., Yang, C., and Sun, B., "A novel mechanism model of the fluidized bed roaster in the zinc roasting process", ***IFAC-PapersOnLine***, 54 (21): 13–18 (2021).

23. Peng, N., Peng, B., Chai, L.-Y., Li, M., Wang, J.-M., Yan, H., and Yuan, Y., "Recovery of iron from zinc calcines by reduction roasting and magnetic separation", ***Minerals Engineering***, 35: 57–60 (2012).

24. Wang, D., Liang, Y., Lin, Z., Peng, C., and Peng, B., "Comprehensive recovery of zinc, iron and copper from copper slag by co-roasting with SO2–O2", ***Journal Of Materials Research And Technology***, 19: 2546–2555 (2022).

25. Hu, W., Xia, H., Pan, D., Wei, X., Li, J., Dai, X., Yang, F., Lu, X., and Wang, H., "Difference of zinc volatility in diverse carrier minerals: The critical limit of blast furnace dust recycle", ***Minerals Engineering***, 116: 24–31 (2018).

26. Gostu, S., Mishra, D., Sahu, K. K., and Agrawal, A., "Precipitation and characterization of zinc borates from hydrometallurgical processing of zinc ash", ***Materials Letters***, 134: 198–201 (2014).

27. Ju, S., Zhang, Y., Zhang, Y., Xue, P., and Wang, Y., "Clean hydrometallurgical route to recover zinc, silver, lead, copper, cadmium and iron from hazardous jarosite residues produced during zinc hydrometallurgy", ***Journal Of Hazardous Materials***, 192 (2): 554–558 (2011).

28. Tiu, G., Ghorbani, Y., Jansson, N., Wanhainen, C., and Bolin, N.-J., "Ore mineral characteristics as rate-limiting factors in sphalerite flotation: Comparison of the mineral chemistry (iron and manganese content), grain size, and liberation", ***Minerals Engineering***, 185: 107705 (2022).

29. Le Gall, M., Choqueuse, D., Le Gac, P.-Y., Davies, P., and Perreux, D., "Novel mechanical characterization method for deep sea buoyancy material under hydrostatic pressure", ***Polymer Testing***, 39: 36–44 (2014).

30. Fontaine, G., Bourbigot, S., and Duquesne, S., "Neutralized flame retardant phosphorus agent: Facile synthesis, reaction to fire in PP and synergy with zinc borate", ***Polymer Degradation And Stability***, 93 (1): 68–76 (2008).

31. Cheng, H., Hou, J., Wang, Y., Zhu, Z., Zhang, Y., Li, X., and Zhang, Y., "Zinc borate modified multifunctional ceramic diaphragms for lithium-ion battery", ***Ceramics International***, 48 (17): 24811–24821 (2022).

32. Zhou, H., Wen, D., Hao, X., Chen, C., Zhao, N., Ou, R., and Wang, Q., "Nanostructured multifunctional wood hybrids fabricated via in situ mineralization of zinc borate in hierarchical wood structures", ***Chemical Engineering Journal***, 451: 138308 (2023).

33. Furuno, T., Wada, F., and Yusuf, S., "Biological resistance of wood treated with zinc and copper metaborates", 60 (1): 104–109 (2006).

34. Heuser, L., Nofz, M., and Müller, R., "Alkali and alkaline earth zinc and lead borate glasses: Sintering and crystallization", ***Journal Of Non-Crystalline Solids: X***, 15: 100116 (2022).

35. Zhu, A., Chen, J., Zhang, Y., and Su, Z., "Cs2B4O5(OH)4: A new hydrated borate with a short UV cutoff edge", ***Inorganica Chimica Acta***, 121252 (2022).

36. Özkul, C., Çiftçi, E., Tokel, S., and Savaş, M., "Boron as an exploration tool for terrestrial borate deposits: A soil geochemical study in Neogene Emet-Hisarcık basin where the world largest borate deposits occur (Kütahya-western Turkey)", ***Journal Of Geochemical Exploration***, 173: 31–51 (2017).

37. Barthélemy, A., Dabringhaus, P., Jacob, E., Koger, H., Röhner, D., Schmitt, M., Sellin, M., and Ingo, K., "Chemistry with weakly coordinating aluminates [Al(ORF)4]− and borates [B(ORF)4]−: From fundamentals to application", Reference Module in Chemistry, Molecular Sciences and Chemical Engineering, ***Elsevier***, (2022).

38. Samyn, F., Bourbigot, S., Duquesne, S., and Delobel, R., "Effect of zinc borate on the thermal degradation of ammonium polyphosphate", ***Thermochimica Acta***, 456 (2): 134–144 (2007).

39. Gostu, S., Mishra, D., Sahu, K. K., and Agrawal, A., "Precipitation and characterization of zinc borates from hydrometallurgical processing of zinc ash", Materials Letters, 134: 198–201 (2014).

40. Peng, Z.-K., Peng, Q.-M., and Ma, Y.-Q., "Thermal characteristics of borates and its indication for endogenous borate deposits", ***Ore Geology Reviews***, 145: 104887 (2022).

41. D s, A. and Vizhi, R. E., "Preparation, structural, optical and thermal behavior of nonlinear Potassium DL-malato borate hydrate (C8H8BKO10H2O) single crystal", ***Journal Of Molecular Structure***, 1248: 131426 (2022).

42. Kołodziejczak-Radzimska, A. and Jesionowski, T., "Zinc Oxide—From Synthesis to Application: A Review", ***Materials***, 7 (4): 2833–2881 (2014).

43. Joseph, M., Nampoori, V. P. N., and Kailasnath, M., "Biofunctionalized zinc oxide nanoflowers coated textiles for UV protection", ***Materials Today: Proceedings***, (2022).

44. Gontrani, L., Donia, D. T., Maria Bauer, E., Tagliatesta, P., and Carbone, M., "Novel Synthesis of Zinc Oxide Nanoparticles from Type IV Deep Eutectic Solvents", ***Inorganica Chimica Acta***, 545: 121268 (2023).

45. Prakash, V., Rai, P., Sharma, N. C., Singh, V. P., Tripathi, D. K., Sharma, S., and Sahi, S., "Application of zinc oxide nanoparticles as fertilizer boosts growth in rice plant and alleviates chromium stress by regulating genes involved in oxidative stress", ***Chemosphere***, 303: 134554 (2022).

46. Sarathi, R., Sheeba, N. L., Selva Essaki, E., and Sundar, S. M., "Titanium doped Zinc Oxide nanoparticles: A study of structural and optical properties for photocatalytic applications", ***Materials Today: Proceedings***, 64: 1859–1863 (2022).

47. Wei, T., Zhang, N., Ji, Y., Zhang, J., Zhu, Y., and Yi, T., "Nanosized zinc oxides-based materials for electrochemical energy storage and conversion: Batteries and supercapacitors", ***Chinese Chemical Letters***, 33 (2): 714–729 (2022).

48. Rajan, A. K. and Cindrella, L., "W-ZnO nanostructures with distinct morphologies: Properties and integration into dye sensitized solar cells", ***Ceramics International***, 46 (6): 8174–8184 (2020).

49. Ali, A., Phull, A.-R., and Zia, M., "Elemental zinc to zinc nanoparticles: is ZnO NPs crucial for life? Synthesis, toxicological, and environmental concerns", Nanotechnology Reviews, 7 (5): 413–441 (2018)

50. Kiomarsipour, N. and Shoja Razavi, R., "Hydrothermal synthesis of ZnO nanopigments with high UV absorption and vis/NIR reflectance", ***Ceramics International***, 40 (7, Part B): 11261–11268 (2014).

51. Bindheim, V., II, "On the different kinds of cadmia, and particularly those of zinc and cobalt", ***The Philosophical Magazine***, 250–255 (1799).

52. Schmidt-Mende, L. and MacManus-Driscoll, J. L., "ZnO – nanostructures, defects, and devices", ***Materials Today***, 10 (5): 40–48 (2007).

53. Al-Hadeethi, Y., Sayyed, M. I., and Rammah, Y. S., "Investigations of the physical, structural, optical and gamma-rays shielding features of B2O3 – Bi2O3 – ZnO – CaO glasses", ***Ceramics International***, 45 (16): 20724–20732 (2019).

54. Catlow, C. R. A., French, S. A., Sokol, A. A., Al-Sunaidi, A. A., and Woodley, S. M., "Zinc oxide: A case study in contemporary computational solid state chemistry", ***Journal Of Computational Chemistry***, 29 (13): 2234–2249 (2008).

55. Santi, C., Tidei, C., Sancineto, L., Bagnoli, L., Marini, F., and Santi, C., "PhSZn-Halides: New Green Thiolates", (2013).

56. "CRC Handbook of Chemistry and Physics", 97. Ed., ***CRC Press***, Boca Raton, 2670 (2016).

57. Yamabi, S. and Imai, H., "Growth conditions for wurtzite zinc oxide films in aqueous solutions", ***Journal Of Materials Chemistry***, 12 (12): 3773–3778 (2002).

58. Zuo, X., Yoon, S.-D., Yang, A., Duan, W.-H., Vittoria, C., and Harris, V. G., "Ferromagnetism in pure wurtzite zinc oxide", ***Journal Of Applied Physics***, 105 (7): 07C508 (2009).

59. Plater, M. J., Foreman, M. R. S. J., Gelbrich, T., and Hursthouse, M. B., "Synthesis and characterisation of infinite di- and tri-nuclear zinc co-ordination networks with flexible dipyridyl ligands", ***Journal Of The Chemical Society, Dalton Transactions***, (13): 1995–2000 (2000).

60. Osmond, G., "Zinc white: a review of zinc oxide pigment properties and implications for stability in oil-based paintings", ***AICCM Bulletin***, 33 (1): 20–29 (2012).

61. Shivashakarappa, K., Reddy, V., Tupakula, V. K., Farnian, A., Vuppula, A., and Gunnaiah, R., "Nanotechnology for the detection of plant pathogens", ***Plant Nano Biology***, 2: 100018 (2022).

62. Tatrari, G., Tewari, C., Pathak, M., Karakoti, M., Bohra, B. S., Pandey, S., SanthiBhushan, B., Srivastava, A., Rana, S., and Sahoo, N. G., "Bulk production of zinc doped reduced graphene oxide from tire waste for supercapacitor application: Computation and experimental analysis", ***Journal Of Energy Storage***, 53: 105098 (2022).

63. Marella, S., Nirmal Kumar, A. R., and Tollamadugu, N. V. K. V. P., "Chapter 19 - Nanotechnology-based innovative technologies for high agricultural productivity: Opportunities, challenges, and future perspectives", Recent Developments in Applied Microbiology and Biochemistry, ***Academic Press***, 211–220 (2021).

64. Sajid, M., "Nanomaterials: types, properties, recent advances, and toxicity concerns", ***Current Opinion In Environmental Science & Health***, 25: 100319 (2022).

65. Prakash Sharma, V., Sharma, U., Chattopadhyay, M., and Shukla, V. N., "Advance Applications of Nanomaterials: A Review", ***Materials Today: Proceedings***, 5 (2, Part 1): 6376–6380 (2018).

66. "1-S2.0-S2352152X22016516-Gr6_lrg.Jpg (3160×1804)", **https://ars.els-cdn.com/content/image/1-s2.0-S2352152X22016516-gr6_lrg.jpg** (2022).

67. Sarabi, G. A. and Bagherzadeh, R., "7 - Conductive nanofibrous materials for supercapacitors", Engineered Polymeric Fibrous Materials, Woodhead Publishing, 157–170 (2021).

68. Guney, M. S. and Tepe, Y., "Classification and assessment of energy storage systems", ***Renewable And Sustainable Energy Reviews***, 75: 1187–1197 (2017).

69. AL Shaqsi, A. Z., Sopian, K., and Al-Hinai, A., "Review of energy storage services, applications, limitations, and benefits", ***Energy Reports***, 6: 288–306 (2020).

70. Hou, T., Fang, R., Yang, D., Zhang, W., and Tang, J., "Energy storage system optimization based on a multi-time scale decomposition-coordination algorithm for wind-ESS systems", ***Sustainable Energy Technologies And Assessments***, 49: 101645 (2022).

71. Wang, Z., Zhang, L., Tang, W., Chen, Y., and Shen, C., "Equilibrium allocation strategy of multiple ESSs considering the economics and restoration capability in DNs", ***Applied Energy***, 306: 118019 (2022).

72. Kurra, N. and Jiang, Q., "18 - Supercapacitors", Storing Energy (Second Edition), ***Elsevier***, 383–417 (2022).

73. Adil, M., Abdelkareem, M. A., Sayed, E. T., Rodriguez, C., Ramadan, M., and Olabi, A.-G., "Progress of Metal Chalcogenides in Supercapacitors", Encyclopedia of Smart Materials, ***Elsevier***, Oxford, 424–433 (2022).

74. Adetokun, B. B., Oghorada, O., and Abubakar, S. J., "Superconducting magnetic energy storage systems: Prospects and challenges for renewable energy applications", ***Journal Of Energy Storage***, 55: 105663 (2022).

75. Rout, C. S. and Late, D. J., "Chapter 1 - Introduction", Fundamentals and Supercapacitor Applications of 2D Materials, ***Elsevier***, 1–10 (2021).

76. Kurzweil, P., "CAPACITORS | Electrochemical Double-Layer Capacitors", Encyclopedia of Electrochemical Power Sources, ***Elsevier***, Amsterdam, 607–633 (2009).

77. Wang, G., Zhang, L., and Zhang, J., "A review of electrode materials for electrochemical supercapacitors", ***Chem. Soc. Rev.***, 41 (2): 797–828 (2012).

78. Sarabi, G. A. and Bagherzadeh, R., "7 - Conductive nanofibrous materials for supercapacitors", Engineered Polymeric Fibrous Materials, ***Woodhead Publishing***, 157–170 (2021).

79. Li, M., Addad, A., Roussel, P., Szunerits, S., and Boukherroub, R., "High performance flexible hybrid supercapacitors based on nickel hydroxide deposited on copper oxide supported by copper foam for a sunlight-powered rechargeable energy storage system", ***Journal Of Colloid And Interface Science***, 579: 520–530 (2020).

80. Raut, S. S. and Sankapal, B. R., "First report on synthesis of ZnFe2O4 thin film using successive ionic layer adsorption and reaction: Approach towards solid-state symmetric supercapacitor device", ***Electrochimica Acta***, 198: 203–211 (2016).

81. Arvas, M. B., Gürsu, H., Gencten, M., and Sahin, Y., "Supercapacitor applications of novel phosphorus doped graphene-based electrodes", ***Journal Of Energy Storage***, 55: 105766 (2022).

82. Yang, Y., Li, S., Li, S., Si, P., and Ci, L., "High-performance hybrid supercapacitor enabled by advantageous heterojunction boosted starfish-like ZnCo-S electrode", ***Journal Of Alloys And Compounds***, 928: 166997 (2022).

83. Sheng, J., "Vitrification of borate waste from nuclear power plant using coal fly ash. (II) Leaching behavior of the FA30 glass", ***Fuel***, 81 (2): 253–256 (2002).

84. Tascioglu, C., Umemura, K., and Yoshimura, T., "Seventh-year durability evaluation of zinc borate incorporated wood-plastic composites and particleboard", ***Composites Part B: Engineering***, 137: 123–128 (2018).

85. Beniwal, R., Gawas, P., Prabha Charan, C., Nutalapati, V., and Murali Krishna Mariserla, B., "Effect of hydroxy groups on nonlinear optical behaviour of encapsulated freebase porphyrin thin films in a borate glass matrix", ***Materials Science And Engineering: B***, 284: 115908 (2022).

86. Chiu, K., Shang, S., Wang, Y., and Jiang, S., "A novel template-free wet chemical synthesis method for economical production of zinc oxide microrods

under atmospheric pressure", ***Ceramics International***, 46 (2): 2002–2009 (2020).

87. Dasta, P., Pratap Singh, A., and Pratap Singh, A., "Zinc oxide nanoparticle as a heterogeneous catalyst in generation of biodiesel", ***Materials Today: Proceedings***, 52: 751–757 (2022).

88. Kuang, D., Liu, L., Mead, J. L., Deng, L., Luo, H., and Wang, S., "Facile synthesis and excellent microwave absorption performance of ultra-small ZnO-doped onion-like carbon nanoparticles", ***Materials Research Bulletin***, 157: 112007 (2023).

89. Yang, S., Guo, X., Chen, P., Xu, D., Qiu, H., and Zhu, X., "Two-step synthesis of self-assembled 3D graphene/shuttle-shaped zinc oxide (ZnO) nanocomposites for high-performance microwave absorption", ***Journal Of Alloys And Compounds***, 797: 1310–1319 (2019).

90. Zheng, X., Sun, Y., Yan, X., Sun, X., Zhang, G., Zhang, Q., Jiang, Y., Gao, W., and Zhang, Y., "High carrier concentration ZnO nanowire arrays for binder-free conductive support of supercapacitors electrodes by Al doping", ***Journal Of Colloid And Interface Science***, 484: 155–161 (2016).

91. Phetcharee, K., Pholauyphon, W., Kwamman, T., Sirisit, N., Manyam, J., and Paoprasert, P., "Enhancing specific capacitance and cycling stability of zinc oxide-based supercapacitors using gamma-irradiated, amine-passivated carbon dots", ***Journal Of Alloys And Compounds***, 933: 167631 (2023).

92. Wang, Q., Han, C., Tang, G., Liu, L., Li, T., and Han, Y., "Preparation of ZnCo-MOF/PPy/Ag2O ternary composites for high-performance flexible supercapacitors", ***Journal Of Alloys And Compounds***, 931: 167510 (2023).

93. Kumar, A., "Sol gel synthesis of zinc oxide nanoparticles and their application as nano-composite electrode material for supercapacitor", ***Journal Of Molecular Structure***, 1220: 128654 (2020).

94. Alver, Ü., Tanrıverdi, A., and Akgül, Ö., "Hydrothermal preparation of ZnO electrodes synthesized from different precursors for electrochemical supercapacitors", ***Synthetic Metals***, 211: 30–34 (2016).

95. Tugrul, N., Bardakci, M., and Ozturk, E., "Synthesis of hydrophobic nanostructured zinc borate from zinc carbonate, and characterization of the product", ***Research On Chemical Intermediates***, 41 (7): 4395–4403 (2015).

96. Bi, Z., Lai, B., Zhao, Y., and Yan, L., "Fast Disassembly of Lignocellulosic Biomass to Lignin and Sugars by Molten Salt Hydrate at Low Temperature for Overall Biorefinery", ***ACS Omega***, 3 (3): 2984–2993 (2018).

97. Shaheen, I., Ahmad, K. S., Zequine, C., Gupta, R. K., Thomas, A. G., and Azad Malik, M., "Sustainable synthesis of organic framework-derived ZnO nanoparticles for fabrication of supercapacitor electrode", ***Environmental Technology***, 43 (4): 605–616 (2022).

98. Li, J. Y., Chen, X. L., Li, H., He, M., and Qiao, Z. Y., "Fabrication of zinc oxide nanorods", ***Journal Of Crystal Growth***, 233 (1): 5–7 (2001).

99. Dai, Y., Zhang, Y., Li, Q. K., and Nan, C. W., "Synthesis and optical properties of tetrapod-like zinc oxide nanorods", ***Chemical Physics Letters***, 358 (1): 83–86 (2002).

100. Kavil, J., M. Anjana, P., Periyat, P., and B. Rakhi, R., "One-pot synthesis of g-C 3 N 4 /MnO 2 and g-C 3 N 4 /SnO 2 hybrid nanocomposites for supercapacitor applications", ***Sustainable Energy & Fuels***, 2 (10): 2244–2251 (2018).

101. Thiagarajan, K., Bavani, T., Arunachalam, P., Lee, S. J., Theerthagiri, J., Madhavan, J., Pollet, B. G., and Choi, M. Y., "Nanofiber NiMoO4/g-C3N4 Composite Electrode Materials for Redox Supercapacitor Applications", ***Nanomaterials***, 10 (2): 392 (2020).

102. Polat, S. and Faris, D., "Fabrication of CuFe2O4@g-C3N4@GNPs nanocomposites as anode material for supercapacitor applications", ***Ceramics International***, 48 (17): 24609–24618 (2022).

103. Mashrah, M. and Polat, S., "Hydrothermal synthesis and electrochemical performance of GNPs-doped MgFe2O4 electrodes for supercapacitors", ***Solid State Ionics***, 391: 116107 (2023).

104. Polat, S. and Mashrah, M., "Synthesis and electrochemical performance of MgFe2O4 with g-C3N4 on Ni-foam as composite anode material in

supercapacitors", ***Journal Of Materials Science: Materials In Electronics***, 33 (30): 23427–23436 (2022).

105. Chandel, M., Moitra, D., Makkar, P., Sinha, H., Singh Hora, H., and Nath Ghosh, N., "Synthesis of multifunctional CuFe 2 O 4 –reduced graphene oxide nanocomposite: an efficient magnetically separable catalyst as well as high performance supercapacitor and first-principles calculations of its electronic structures", ***RSC Advances***, 8 (49): 27725–27739 (2018).

106. Najib, S., Bakan, F., Abdullayeva, N., Bahariqushchi, R., Kasap, S., Franzò, G., Sankir, M., Sankir, N. D., Mirabella, S., and Erdem, E., "Tailoring morphology to control defect structures in ZnO electrodes for high-performance supercapacitor devices", ***Nanoscale***, 12 (30): 16162–16172 (2020).

107. Wang, G., Zhang, L., and Zhang, J., "A review of electrode materials for electrochemical supercapacitors", ***Chemical Society Reviews***, 41 (2): 797–828 (2012).

108. Saranya, M., Ramachandran, R., and Wang, F., "Graphene-zinc oxide (G-ZnO) nanocomposite for electrochemical supercapacitor applications", ***Journal Of Science: Advanced Materials And Devices***, 1 (4): 454–460 (2016).

109. Pang, H., Ma, Y., Li, G., Chen, J., Zhang, J., Zheng, H., and Du, W., "Facile synthesis of porous ZnO–NiO composite micropolyhedrons and their application for high power supercapacitor electrode materials", ***Dalton Transactions***, 41 (43): 13284–13291 (2012).

110. Cai, D., Huang, H., Wang, D., Liu, B., Wang, L., Liu, Y., Li, Q., and Wang, T., "High-Performance Supercapacitor Electrode Based on the Unique ZnO@Co3O4 Core/Shell Heterostructures on Nickel Foam", ***ACS Applied Materials & Interfaces***, 6 (18): 15905–15912 (2014).

## RESUME

Chikh Sidi El Mokhtar Sidi Mohamed LEFDHİL has completed his primary, secondary, and undergraduate education in Mauritania. He graduated from El Taghwa School in Nouakchott in 2016 and then attended the University of Nouakchott Al Asriya, where he graduated in 2019 with a degree in geological science. He then went on to pursue a master's degree in Metallurgy and Material Engineering at Karabuk University's (Institute of Applied Science) and graduated in 2022.